Title
BMP signaling is required for cell cleavage in preimplantation-mouse embryos.

Journal
Developmental biology, 397(1)

ISSN
0012-1606

Authors
Reyes de Mochel, Nabora Soledad
Luong, Mui
Chiang, Michael
et al.

Publication Date
2015

DOI
10.1016/j.ydbio.2014.10.001

Peer reviewed

Developmental Biology 397 (2015) 45–55

Contents lists available at ScienceDirect

Developmental Biology

journal homepage: www.elsevier.com/locate/developmentalbiology

BMP signaling is required for cell cleavage in preimplantation-mouse embryos

Nabora Soledad Reyes de Mochel [a], Mui Luong [a], Michael Chiang [a], Anna L. Javier [a], Elizabeth Luu [a], Toshihiko Fujimori [b], Grant R. MacGregor [a], Olivier Cinquin [a], Ken W.Y. Cho [a,*]

[a] Department of Developmental & Cell Biology, University of California, Irvine, CA 92697-2300 USA
[b] Division of Embryology, National Institute for Basic Biology, Aichi, Japan

ARTICLE INFO

Article history:
Received 16 July 2014
Received in revised form
3 October 2014
Accepted 4 October 2014
Available online 14 October 2014

Keywords:
BMP
Smad1
Morula
Preimplantation
Cell cleavage
Cell division

ABSTRACT

The mechanisms regulating cell division during development of the mouse pre-implantation embryo are poorly understood. We have investigated whether bone morphogenetic protein (BMP) signaling is involved in controlling cell cycle during mouse pre-implantation development. We mapped and quantitated the dynamic activities of BMP signaling through high-resolution immunofluorescence imaging combined with a 3D segmentation method. Immunostaining for phosphorylated Smad1/5/8 shows that BMP signaling is activated in mouse embryos as early as the 4-cell stage, and becomes spatially restricted by late blastocyst stage. Perturbation of BMP signaling in preimplantation mouse embryos, whether by treatment with a small molecule inhibitor, with Noggin protein, or by over-expression of a dominant-negative BMP receptor, indicates that BMPs regulate cell cleavage up to the morula stage. These results indicate that BMP signaling is active during mouse pre-implantation development and is required for cell cleavage in preimplantation mouse embryos.

Introduction

Mammalian pre-implantation development has been best studied in the mouse. After fertilization, mammalian embryos undergo four rounds of cell division to reach the morula stage, a solid ball of approximately 16 cells. Cells on the inside of the morula differ from those on the outside in several ways including genes expressed, cell shape, and cell adhesion characteristics (Ziomek et al., 1982; Zernicka-Goetz et al., 2009; Rossant and Tam, 2009). Subsequently, a combination of symmetric and asymmetric cell divisions and cavitation transforms the morula into a blastocyst (32-cell stage) (Smith and McLaren, 1977). The blastocyst hatches from the zona pellucida in preparation for implantation at around embryonic day E 4.5.

Inner cell mass (ICM) and trophectoderm (TE) cell differentiation is promoted by several transcription factors (TFs) that are expressed dynamically during this developmental transition. *Pou5f1/Oct4*, *Nanog*, and *Sox2* specify ICM cells while *Tead4* and *Cdx2* specify TE cells (Nichols et al., 1998; Avilion et al., 2003; Chambers et al., 2003; Strumpf et al., 2005; Wang and Dey, 2006; Yagi et al., 2007; Nishioka et al., 2008). TE cells can be further characterized by their location relative to the ICM as polar and mural TE cells. Polar TE cells are defined as those that overlay the ICM while the mural TE cells overlay the blastocoel cavity, with division of polar TE contributing cells to the mural TE compartment (Copp, 1978; Gardner and Davies, 2002). The essential roles of TFs such as *Pou5f1/Oct4*, *Nanog*, *Sox2*, *Tead4* and *Cdx2* in specifying ICM and TE lineages have been extensively studied. In contrast, our understanding of how cell division is regulated during pre-implantation development is relatively limited (Ciemerych and Sicinski, 2005).

Recent single cell RNA-seq expression profiling (Tang et al., 2010) indicates BMP signaling components, including BMP ligands, receptors, and Smads, are all expressed in early stages of mouse pre-implantation development (Fig. S1). This raises the possibility that BMP signaling may function during mouse pre-implantation development. Mouse mutants deficient in various BMP ligands, intracellular transducers, and receptors have underscored the importance of BMP signaling during gastrulation; *e.g.* Mishina et al. (1995), Macías-Silva et al. (1998), Solloway and Robertson (1999), Yi Se et al. (2009), Arnold et al. (2006), but has thus far failed to disclose a role(s) for BMP signaling at pre-implantation stages, possibly because of redundancies in BMP signaling that ensure the robustness of embryonic developmental programs. Smad1 and 5 single homozygous null mice have similar phenotypes as the Smad1$^{+/-}$: Smad5$^{+/-}$ double heterozygous mutants presumably because they are functionally redundant (Arnold et al., 2006). An

* Corresponding author.

http://dx.doi.org/10.1016/j.ydbio.2014.10.001
0012-1606/

inability to generate Smad1 and 5 homozygous null mice precluded genetic analysis of a role for BMP signaling in pre-implantation mouse development, illustrating the challenge of investigating the function of BMP signaling pathway components in development. Mice deficient in BMP type I receptor (BMPr1a/ALK3) or type II receptor (BMPrII/BMPR2), however, were smaller and had fewer cells (Beppu et al. 2000; Mishina et al. 1995), supporting a potential involvement of BMP signaling in cell proliferation. Coucouvanis and Martin (1999) used *in situ* hybridization to demonstrate that *Bmp4* RNA is present exclusively in the ICM cells of the blastocyst. They also used *in vitro* culture of embryoid bodies made from aggregated PSA1 embryonal carcinoma cells to demonstrate that inhibition of BMP via expression of a dominant negative *Bmpr-Ib* blocked both cavitation and expression of *Hnf4a*, a marker of visceral endoderm.

To investigate if BMP signaling functions in mouse preimplantation embryonic development, we measured the direct output of BMP signaling during this period using two different approaches. The first method examines the transcriptional response of "BMP-indicator" mouse embryos, while the second measured the status of Smad1/5/8 phosphorylation within preimplantation stage embryos. We mapped and quantitated the dynamic activities of BMP signaling through high-resolution immunofluorescence imaging combined with a 3D segmentation method. We find that BMP signaling activity can be detected in all blastomeres as early as the 4-cell stage (E2.0) and becomes spatially restricted by late blastocyst stage. Perturbation of BMP signaling in embryos, by treatment with a pharmacologic inhibitor, by Noggin protein, or by overexpression of a dominant-negative BMP receptor, each delayed cell cleavage during early cleavage stages. Based on these results, we propose that BMP signaling is required for normal cell cycle during development of the preimplantation mouse embryo.

Results

BMP signaling activity in preimplantation embryos revealed by BRE-gal expression and the phosphorylation state of Smad1/5/8

We investigated for evidence of BMP activity during mouse preimplantation development using mice transgenic for a BMP-dependent *lacZ* reporter gene (BRE-gal) (Javier et al., 2012). BMP-responsive elements (BRE) are *cis*-acting sequences that respond to canonical Smad-dependent BMP signaling in the frog *Xenopus* (von Bubnoff et al., 2005), *Drosophila* (Yao et al., 2006), zebrafish (Alexander et al., 2011), and mouse (Javier et al., 2012; Doan et al., 2012). A BRE element was adapted to generate a BMP-dependent reporter gene by placing seven copies of the BRE in tandem upstream of a *X. laevis Id3*-gene minimal promoter:: *nlsLacZ* reporter gene (Maretto et al., 2003). BRE-gal mice identified SMAD-dependent BMP activity in E5.5 to E13.5 post-implantation stage mouse embryos (Javier et al., 2012; Doan et al., 2012). We used BRE-gal mice to analyze BMP signaling in the pre-implantation mouse embryo from morula (~E2.5) to blastocyst (~E3.5) stage (Fig. 1A). Nuclear β-gal activity was observed in both ICM and TE of blastocysts, although the activity in ICM was in general stronger than that observed in TE. To provide independent evidence that BMP signaling is active in the blastocyst, immunofluorescence analysis was performed to identify the phosphorylated form of Smad1/5/8 (hereafter referred to as p-Smad1), produced by receptor-activated BMP signaling. Phospho-Smad1 was detected in all nuclei of the E3.5 stage embryo (Fig. 1B). The difference in cellular patterns of X-gal staining (enriched expression in ICM) and p-Smad1 immunostaining (uniform expression) may be due to reduced sensitivity of the BRE-gal reporter compared to anti-pSmad1 staining. Alternatively, although both ICM and TE cells receive BMP signaling, the transcriptional machinery mediating BMP signaling in these lineages may differ, with only a subset of this activity being detected by the BRE-gal reporter construct. Immunostaining using a pan-Smad1 antibody showed predominantly cytoplasmic localization of Smad1 (Fig. 1C) suggesting that the majority of Smad1 present in the preimplantation stage embryos is unphosphorylated. This suggests that the availability of Smad1 is not rate limiting in regulating BMP signaling activity in the preimplantation stage mouse embryo.

Specificity of the p-Smad1 antibody was verified using E14Tg2a mouse embryonic stem (mES) cells. Following stimulation with BMP4 the mES cells show p-Smad1 staining within the nucleus, which was inhibited in the presence of either Noggin or a small molecule BMP antagonist LDN193189 (4-(6-(4-(piperazin-1-yl)phenyl)pyrazolo[1,5-a]pyrimidin-3-yl)quinoline hydrochloride) (Fig. S2A; Vogt et al., 2011). X-gal staining of BRE-gal ES cells also shows that BRE-gal induction was dependent on BMP signaling (Fig. S2B). Western blot analysis of total protein from treated mES cells also detected p-Smad1 upon stimulation with BMP4, which was prevented in the presence of LDN193189 (Fig. S2C). LDN193189 is a highly selective antagonist of the intracellular kinase domain of the BMP receptor isotypes ALK2 (activin receptor-like kinase 2, also known as ACVR1), ALK3 (BMPR1A) and ALK6 (BMPR1B) (Yu et al., 2008; Cuny et al., 2008). We also examined the effect of LDN193189 on the transcriptional response of known BMP-target genes and found that the inhibitor effectively down-regulated expression of *Id1*, *Id2* and *Id3* (Hollnagel et al., 1999) (Fig. S2D). Taken together, our data support that p-Smad1 staining in E3.5 mouse blastocysts is specific and that LDN193189 is an effective BMP antagonist.

BMP signaling is detected as early as the four-cell stage of mouse development

We determined the earliest stage at which p-Smad1 staining is detectable in preimplantation stage mouse embryos. Phospho-Smad1 staining is below the limit of detection in the 2-cell stage embryo, but is detected at the 4-cell stage and persists through late blastocyst (~100-cell stage) (Fig. 1D and E). The onset of p-Smad1 staining precedes the appearance of X-gal staining in the BRE-gal embryos, the latter first being detected at around the 16-cell morula stage (Fig. 1A). The observed delay in X-gal staining (Fig. 1A) could be explained by a required threshold concentration of p-Smad1 to activate the BRE-gal reporter gene or that the BRE-gal reporter is not responsive to all BMP signaling events. Based on these results, we conclude that BMP signaling is activated by the 4-cell stage, prior to known activation of transcription factors including *Cdx2*, *Nanog*, *Tead4* and *Pou5f1/Oct4* that are required to establish the transcriptional network for ICM and TE cell lineage selections (Nichols et al., 1998; Avilion et al., 2003; Chambers et al., 2003).

Confocal imaging (Fig. 1F) revealed a non-uniform, punctate staining of p-Smad1 predominantly within the nucleus, but absent from the nucleolus. Nucleoli were identified by absence of Hoechst staining within the nucleus (Martin et al., 2005). This punctate staining can be detected as early as 4-cell stage (~E2.0) and persists until the blastocyst stage (E3.5–4.5). Similar punctate p-Smad1-staining pattern has been observed in other tissues (Eom et al., 2011; Hogg et al., 2010), and may represent transcriptional regulatory complexes.

Increased p-Smad1 in the ICM

We investigated whether average cellular phospho-Smad1 levels changed during early pre-implantation development. To quantitate changes we developed a computer program that segments individual nuclei in three-dimensional confocal stacks (a sample output of an analysis is shown in Fig. 2A, and volume rendering of an embryo in Fig. 2B; see "Experimental procedures" section for more detail and accuracy measurements, Fig. S3A). Mean p-Smad1 levels at the four and eight cell stages were not significantly different ($p=0.16$).

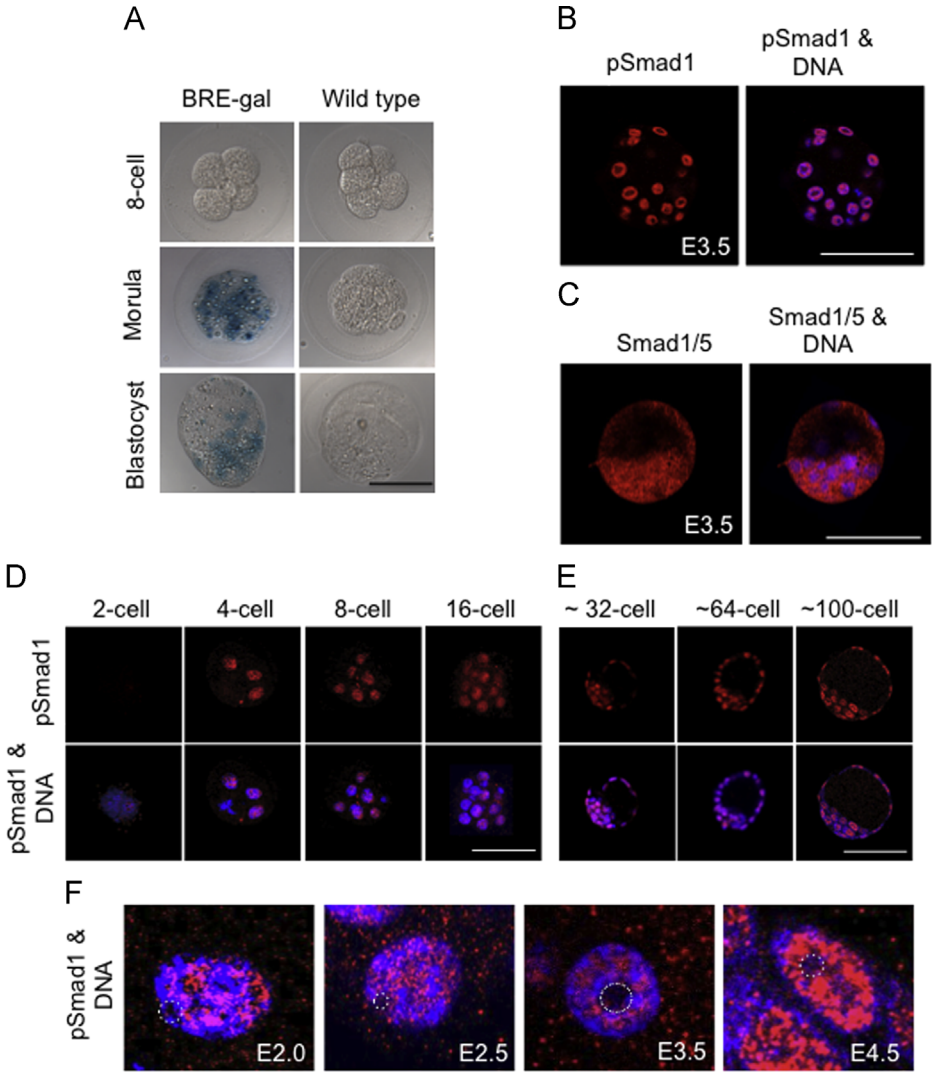

Fig. 1. Bre-gal reporter activity and location of p-Smad1 in preimplantation mouse embryos. (A) Homozygous BRE-gal and CD1 E3.5 mouse embryos (8-cell, morula, and blastocyst stage) stained for β-gal activity using X-gal. X-gal staining is stronger in the ICM compared to the TE of mouse blastocysts. Non-transgenic (wild type) embryos do not show X-gal staining. (B and C) E3.5 mouse embryos immunostained with p-Smad1 and Smad1 antibodies, respectively. (D and E) Timeline of p-Smad1 activity in developing mouse embryos between E1.5 and E4.5 stages (2–100-cell stages). (F) Nuclei of E2.5-E4.5 mouse embryos stained for p-Smad1 and DNA, nucleoli lacking pSmad1 are indicated by white dotted circles. Scale bar = 100 μm.

Likewise, mean p-Smad1 levels remained constant at the 16, 32, and 64-cell stages (Fig. 2C, S3B and C).

Next, we asked whether p-Smad1 levels differed in inner cells *versus* outer cells. To address this question we quantified p-Smad1 levels in manually annotated inner and outer cells using image segmentation (see the "Experimental procedures" section). No significant difference was observed in ~16-cell stage embryos (Fig. 2D left, $p=0.2$, $n=18$, Fig. S3C). In contrast, p-Smad1 levels were enriched in ICM cells at the ~64-cell stage blastocyst (Fig. 2D right, $p<0.001$, $n=13$, Fig. S3C). We also compared p-Smad1 levels in manually annotated polar/mural TE cells, using the embryonic axis and ICM to distinguish the two cell types. At the 64-cell stage, polar TE cells had higher p-Smad1 levels than mural TE cells (Figs. 2E, $p<0.001$; see Fig. 2F for spatial distribution of p-Smad1 in a sample embryo). The observation that ICM cells displayed more intense p-Smad1 staining than TE cells (Fig. 2D, E and Fig. S3D) and that BMP4 was specifically expressed in the ICM cells (Fig. S1), combined with a study of the mitotic index of different regions of the TE (Copp, 1978), suggests secretion of BMP4 from the ICM may influence the mitotic index of TE cells with proximity to a higher local concentration of BMP correlating with higher mitotic index in polar TE *versus* mural TE.

BMP signaling in cell division

To investigate functions of BMP signaling during pre-implantation development, BMP signaling was inhibited using the small molecule BMP antagonist LDN193189. Culture of 8-cell stage embryos in 1 μM LDN193189 for 24 h blocked formation of a blastocoel cavity (Fig. 3A). We verified LDN193189 was blocking BMP signaling with p-Smad1 immunostaining, which was weaker in LDN193189-treated embryos (Fig. 3B, top panels). Similarly, BRE-gal reporter gene activity was also reduced in morula stage embryos treated with LDN193189 (Fig. 3B, bottom panels). We quantified p-Smad1 levels in LDN193189-treated embryos ($n=8$, ~30-cells per embryo) and in sibling control embryos (n = 5, ~54-cells per embryo) using image segmentation (see the "Experimental procedures" section). Mean p-Smad1 levels were reduced in LDN193189-treated embryos (Fig. 3C, $p<0.001$).

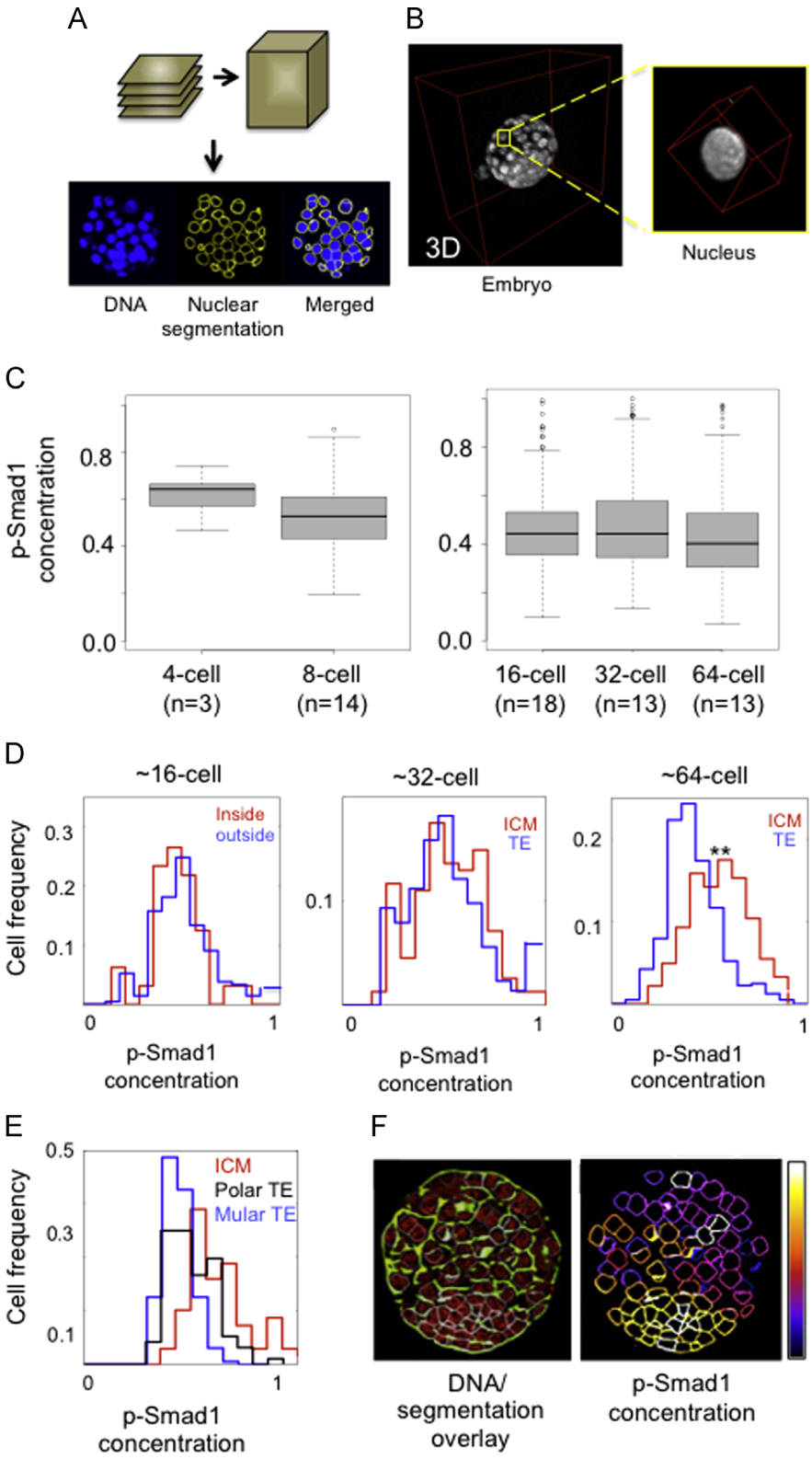

Fig. 2. Distribution of p-Smad1 in preimplantation embryos. (A) Schematic of data acquisition. Z-stacks of each randomly oriented embryo were collected using 63 × objective at 0.3 μm intervals, and subjected to a 3D segmentation approach. DNA in blue (left), segmented nuclei in yellow (middle), and merged image (right). (B) A 3D image of an embryo after segmentation and a magnified nucleus. (C) Nuclear p-Smad1 concentrations in the blastomeres of pre-morula (4–8-cell) and later stage embryos (~16-, 32-, and 64-cell). (D) Distribution of nuclear p-Smad1 concentrations at 16-, 32- and 64-cell stages. p-Smad1 concentrations in inside and outside cells of 16-cell stage embryos are 0.43 and 0.46, respectively. p-Smad1 concentrations in ICM and TE cells of 32-cell stage blastocysts are 0.47 and 0.45, respectively. p-Smad1 concentrations of ICM cells of 64-cell stage embryos (0.49, $n=314$ cells) are notably higher than those in TE cells (0.38, $n=485$ cells, $p<0.001$). (E) p-Smad1 staining levels in ICM ($n=104$ cells), Polar TE ($n=142$ cells), and Mural TE ($n=213$ cells) in ~100-cell stage embryos. (ICM *vs* Polar TE, $p<0.001$; ICM v Mural TE, $p<0.001$; Polar *vs* Mural TE, $p<0.001$). (F) Nuclear p-Smad1 concentration in individual nuclei; ICM is located at the bottom of the embryo shown. Florescence intensity differences were color-coded on segmentation outlines (from low to high: purple, orange, yellow and white). The numerical numbers from 0 to 1 indicate the relative fluorescence intensity range. *p*-values were derived using Student's *t*-test.

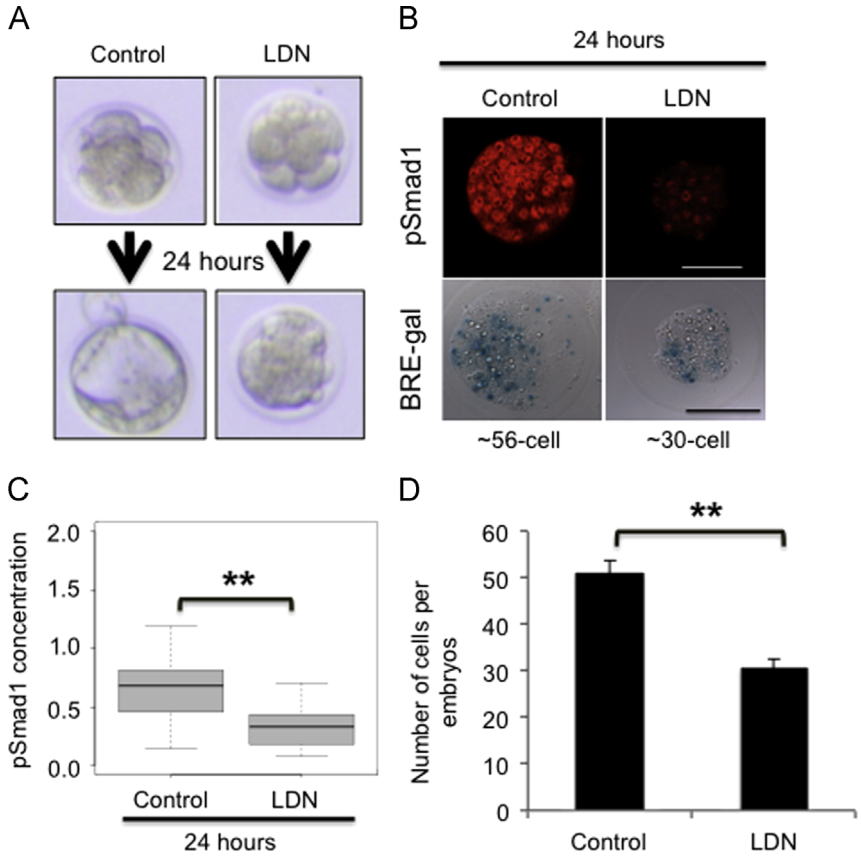

Fig. 3. BMP signaling inhibition affects cell cleavage. (A) Images of embryos collected at E2.5 (pre-compaction, top panels) and incubated with and without LDN193189 for 24 h (bottom panels). (B) Decrease in p-Smad1 and X-gal staining in embryos cultured in LDN193189 for 24 h. Scale = 100 μm. (C) Quantification of p-Smad1 in control ($n=5$, mean concentration of 0.66) and LDN193189-treated ($n=8$, mean concentration of 0.40, $p<0.001$) embryos. The data is reported as nuclear concentration. (D) Decrease in cell numbers in embryos treated with LDN193189. The average numbers of cells are 51 ± 2.5 cells for control ($n=33$) and 30.6 ± 2 cells at 1 μM LDN193189 ($n=38$, $p<0.001$).

LDN193189-treated embryos had fewer cells compared to *in vitro*-cultured control embryos (Fig. 3D, $p<0.001$). Two criteria suggest the reduction in cell number after LDN193189-treatment is not due to increased cell death. The first is absence of DNA condensation and nuclear fragmentation, characteristics of apoptosis (White, 1996), in DNA stained embryos treated with 1 μM LDN193189. Second, apoptosis was not detected in embryos treated with 1 μM LDN193189 ($n=16$) using a TUNEL assay, although at a higher concentration of LDN193189 (2.5 μM), apoptosis could be detected (Fig. S4). These results suggest that inhibition of BMP signaling by 1 μM LDN193189 interferes with normal blastocyst development by reducing mitotic index and not by increasing rate of apoptosis.

We next investigated whether pre-implantation embryos displayed stage-specific sensitivity to LDN193189-mediated inhibition of BMP signaling. Pre-implantation embryos were isolated at different stages (E2.5, E3.0, and E3.5), then cultured *in vitro* for 24 hours in the presence of 1 μM LDN193189 (Fig. 4A). Over 50% of 8-cell embryos ("early morula") cultured in this manner failed to form normal blastocysts (Fig. 4Bb and Bb′), while late morula and blastocyst stage embryos treated with LDN193189 formed morphologically normal blastocysts (Fig. 4B and C). These results identify an important BMP signaling period in 8-cell early embryos and indicate that exposure to 1 μM LDN193189 does not cause death of the embryo. We further determined that LDN193189 treatment for as little as 12 h was sufficient to affect cell cleavage (Fig. S5A). Embryos treated with lower LDN193189 concentrations (0.25 μM) displayed similar, albeit weaker, effects (Fig. S5B). We also cultured LDN193189-treated embryos beyond 24 h. While some embryos failed to develop further, the surviving embryos were able to form blastocysts at later stages, suggesting that BMP signaling inhibition causes developmental delay.

Overexpression of a dominant negative BMP receptor blocks cell cleavage

One concern of using chemical inhibitors is possible non-specific effects of the drug—in this case, inhibition of other ALK family receptors. To obtain independent evidence for a function of BMP signaling in early embryonic cell cleavage, we used a genetic approach. A DNA construct (CMV-DNBR-HA) encoding an epitope-tagged dominant negative type I BMP receptor 1a (BMPR1a/ALK3) was generated (Lim et al., 2004). The ability of this construct to affect BMP signaling was tested in mES cells. As with LDN193189 treatment, expression of CMV-DNBR-HA inhibited phosphorylation of Smad1 upon BMP4 stimulation, (Fig. S6A, lanes 3, 4). To examine the effects of expressing DNBR-HA in embryos, we microinjected CMV-DNBR-HA into a single blastomere of 2-cell stage embryos and analyzed the effect at the 8-cell stage of development (Fig. 5A). The presence of DNBR-HA on the surface membrane of the descendants of injected blastomeres was confirmed by immunostaining (Fig. S6B). The cell number in CMV-DNBR-HA/CMV-β-gal co-injected and control CMV-β-gal injected embryos were quantified after 24 h of *in vitro* culture. Embryos expressing CMV-DNBR-HA/CMV-β-gal had an average of 6.45 ± 0.2 cells, while CMV-β-gal injected embryos had 8.2 ± 0.4 cells. Thus, DNBR-HA expressing embryos have fewer cells than control CMV-β-gal injected embryos (Fig. 5B and C; $p<0.001$), and reduced levels of p-Smad1 staining (Fig. S6C; $p<0.001$). Cell lineage analysis (β-gal expressing cells) also revealed that fewer cells were derived from CMV-DNBR-HA-expressing blas-

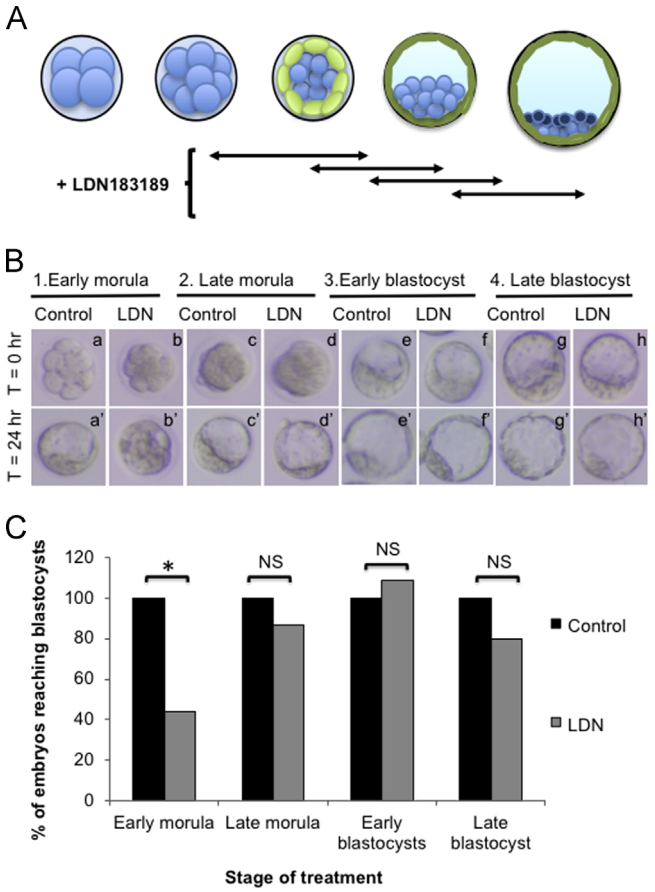

Fig. 4. Temporal limits of LDN193189 sensitivity. Experimental schematic determining the BMP signaling sensitive period. (B) Embryos at early morula (uncompacted), late morula (compacted), early blastocyst (~32-cell) and late blastocyst (~60-cell) stages before (a–h) and 24 h after LDN193189 treatments (a′–h′). (C) Percentages of embryos reaching blastocysts stage (a and a′) $n=37$, (b and b′) $n=52$, (c and c′) $n=72$, (d and d′) $n=60$, (e and e′) $n=14$, (f and f′) $n=13$, (g and g′) $n=48$, (h and h′) $n=46$). $^{*}p<0.05$ based on Student's t test.

tomeres (an average of 2.5 ± 0.1 cells) compared to those contributed from the uninjected control blastomere (contralateral side, 3.7 ± 0.2 cells). We used an additional independent method to inhibit BMP signaling in pre-implantation embryos, by removing the zona pellucida using acid Tyrode's followed by incubation of the 8-cell stage embryos with Noggin protein, a BMP antagonist. Noggin treatment also resulted in developmental delays (Fig. 6D). These results provide independent confirmation that inhibition of BMP signaling affects cell cleavage in preimplantation stage embryos.

Time lapse imaging of LDN193189-treated embryos

To better define the cell cleavage defects seen in mouse embryos after the LDN193189 treatment, we performed time-lapse imaging of CAG:H2B-GFP mouse embryos that express GFP tagged histone H2B in the presence and absence of LDN193189 (Kurotaki et al., 2007). Fig. 5E shows the images of CAG:H2B-GFP e1.5 embryos (2-cell stage) after 60 h of *in vitro* culturing with and without LDN193189. LDN193189-treated embryos (bottom panel) develop significantly slower than the untreated embryos (top panel). We quantified the average cell-cycle time of each cleavage, and found that 2nd, 3rd, 4th and 5th cleavages are all significantly delayed in LDN193189-treated embryos (Fig. 5F). Throughout this experiment, no evidence of apoptosis was detected. Hence, LDN193189-treatment appears to cause an increase in cell cycle time without causing apoptosis.

Inhibition of BMP signaling delays ICM and TE cell segregation

We hypothesized that if BMP signaling is required for blastocyst formation, blockade of BMP signaling by LDN193189 might disrupt ICM and TE cell lineage specification. Nanog and Cdx2 positive cells are present in the morula stage embryo, and by the early blastocyst stage they segregate to mark ICM and TE cells (Dietrich and Hiiragi, 2007). We examined whether inhibiting BMP signaling via LDN193189 alters Nanog and/or Cdx2 expression. Embryos at 8-cell stage were treated with 1 μM LDN193189, cultured *in vitro* for 24 h, and subjected to immunofluorescence staining for the transcription factors Nanog and Cdx2 followed by 3D segmentation (Fig. 6A). As noted previously, LDN193189 treated embryos showed delay in cell cleavage (Fig. 6B). Exposure to LDN193189 caused reduction of Cdx2 in outside cells, while Nanog expression was relatively unaffected (Fig. 6C and D). To determine whether the difference in Cdx2 expression could be a consequence of developmental delay, we compared the expression of Nanog and Cdx2 to that found in cell number matched embryos (~30-cell stage embryo, 12 h control). The relative expression levels of Nanog and Cdx2 were similar suggesting that the difference in gene expression between control and LDN193189-treated embryos is due to developmental delay.

Discussion

We have examined the presence of BMP signaling during development of the preimplantation stage mouse embryo and investigated its function during this process. The results indicate that BMP signaling is active as early as the 4-cell stage of development and is required to regulate rate of cell cleavage up to the morula stage.

Results of experiments using three independent methods provide consistent support for the requirement of BMP signaling during pre-implantation development. Inhibition of BMP signaling by LDN193189 using concentrations up to 1 μM interferes with cell cleavage, but does not cause cell death. Expression of a dominant negative BMPR1a/ALK3 in mosaic embryos, and exposure of whole embryos to the BMP-antagonist Noggin cause similar effects on rate of cell division. Based on these findings we postulate that inhibition of BMP signaling via ALK3 reduces cell number in the blastocyst by increasing cell cycle length. How might BMP signaling influence rate of cell division? BMP signaling can directly control expression of *Id* genes, which encode proteins that heterodimerize with basic helix-loop-helix (bHLH) proteins thereby inhibiting their function. Basic HLH proteins have been implicated in regulation of the cell cycle (von Bubnoff et al., 2005; Massari and Murre, 2000; Murre et al., 1989). *Id2* and *Id3* are differentially expressed in preimplantation stage embryos (Tang et al., 2010; Guo et al., 2010) and forced expression of *Id* genes can bypass the mES cells requirement for BMP for self-renewal (Ying et al., 2003). Hence, regulation of the cell cleavage by BMP signaling might be mediated via differential expression of *Id2* and *Id3*.

Interestingly, BMP signaling can also negatively regulate cell division in the early mouse embryo. Epiblast specific loss of ACVR1/ALK2 affects the ability of ventral cells in the node to enter G_0 (Komatsu et al., 2011). Deletion of ALK2 attenuated the level of stabilized $p27^{Kip1}$ cyclin-dependent kinase inhibitor normally required to inhibit nodal cell proliferation and formation of a primary cilium. Together with the results of the present study, this suggests BMP signaling can have opposite effects on cell cycle in the early mouse embryo depending on the specific BMP signaling pathway and cell type involved.

Signaling through BMP receptors can be transduced via Smad4-dependent canonical (Smad1/5/8) pathways and Smad4-independent

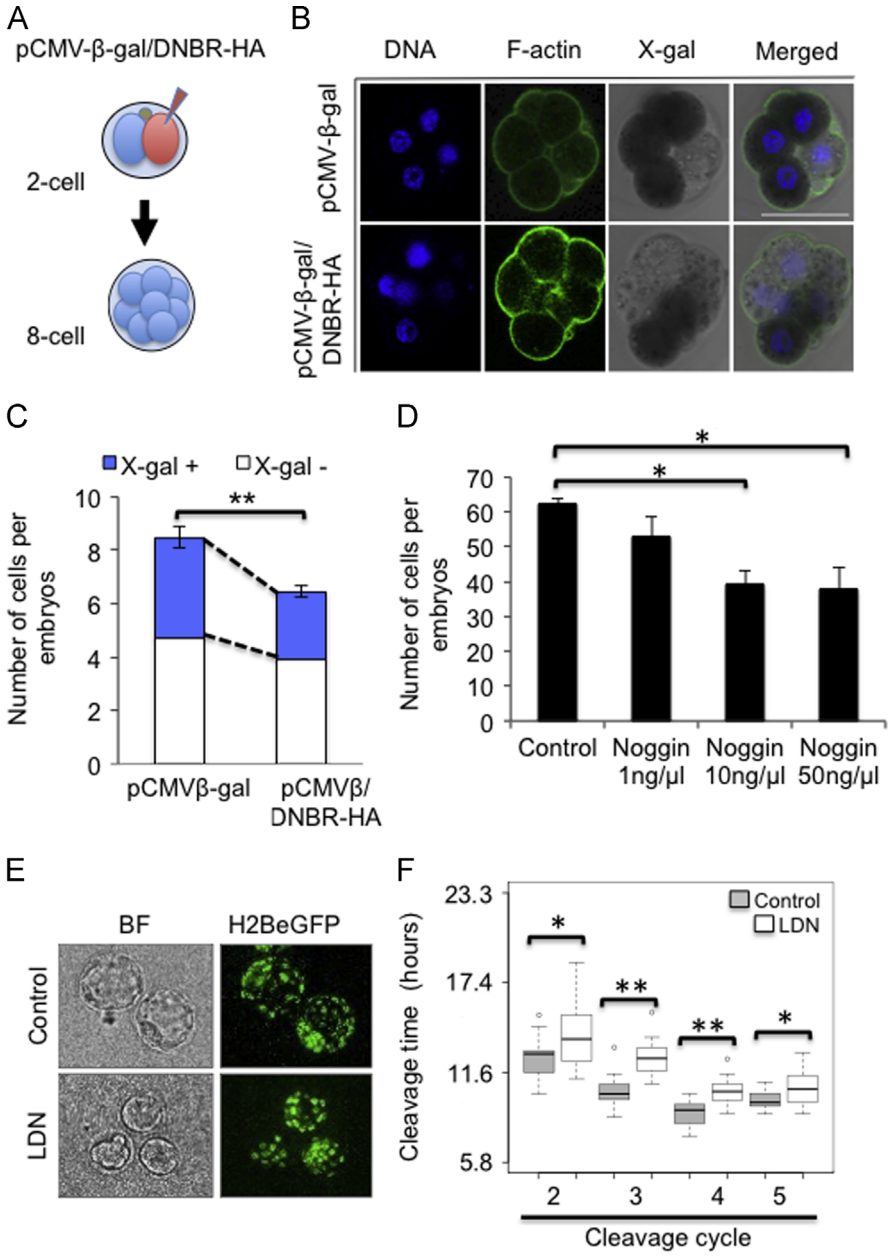

Fig. 5. Dominant-negative BMP receptor overexpression affects cell cleavage. (A) Schematic diagram showing DNA microinjection experiment. (B) Effects of DNBR-HA expression on cell cleavage. CMV-β−gal injected embryos with and without CMV-DNBR-HA were subjected to X-gal staining. Dark grey colored blastomeres in X-gal panels indicate the descendants of CMV-β-gal injected blastomeres. Scale bar=100 μm. (C) Bar graph showing the effects of DNBR-HA on cell cleavage. Average total cell numbers per embryos after pCMVβ and pCMVβ/DNBR-HA injections are 8.4 ± 0.4 cells and 6.45 ± 0.2 cells, respectively. The number of X-gal lineage traced blastomeres for pCMVβ and pCMVβ/DNBR-HA are 3.7 ± 0.2 cells and 2.5 ± 0.1 cells, respectively. For pCMVβ (n=27) and for pCMVβ/DNBR-HA (n=40). (D) Decrease in total cell numbers after Noggin treatment. Total cell numbers after each Noggin treatment are 62.5 ± 1.5 cells (n=3, control), 53.1 ± 5.7 cells (n=7, 1 ng/μl), 39.1 ± 4.1 cells (n=8, 10 ng/μl), and 37.8 ± 6.3 cells (n=9, 50 ng/μl). (E) Images of H2BeGPF with and without LDN193189. (F) LDN193189 treatment delays cell cleavage. Cell cleavage lengths were measured for control (n=14) and LDN treated (n=19) embryos at the 2nd, 3rd, 4th, and 5th, cleavage. $^{*}p<0.05$, $^{**}p<0.001$, BF, bright field. Data are averages ± SEM.

non-canonical (BMP/TGF-β-activated kinase-1, TAK1) pathway Yamaguchi et al., 1999, 1995; Derynck and Zhang, 2003; Moustakas and Heldin, 2005). At present, the relative contribution of these pathways to cell division in preimplantation embryos is not fully understood. Mutation of *Smad4* in mice results in defective gastrulation (Takaku et al., 1998; Chu et al., 2004) although analysis of embryos at preimplantation stages was not reported in these studies. It would be of interest to investigate if *Smad4*-mutant pre-implantation embryos have fewer cells compared to control embryos. BMP signaling might also influence cell division via the TAK1 non-canonical signaling pathway. Smad1 activity can be inhibited by phosphorylation of its linker region by ERK, which results in exclusion of Smad1 from the nucleus (Kretzschmar et al., 1997) and its association with Smurf1 which ubiquitinylates Smad1 leading to its degradation (Fuentealba et al., 2007; Sapkota et al., 2007). TAK1 can maintain Smad1 activity indirectly by inhibiting ERK. The mechanism of inhibition involves p38-dependent activation of a PP2A complex that binds and dephosphorylates MEK and ERK (Westermarck et al., 2001). Interestingly, pre-implantation mouse embryos express all four genetic forms of p38 (α,β,δ,γ) and pharmacologic inhibition of p38 α and β forms can reversibly halt mouse embryo development at the 8–16 cell stage but not before (Natale et al., 2004). Hence, BMP signaling, in part via TAK1, might be required for cell division of mouse embryos following compaction.

BRE-gal ES cells respond well to exogenous BMP stimulation as indicated by strong β-gal activity (Fig. S2B). However, BRE-gal mES

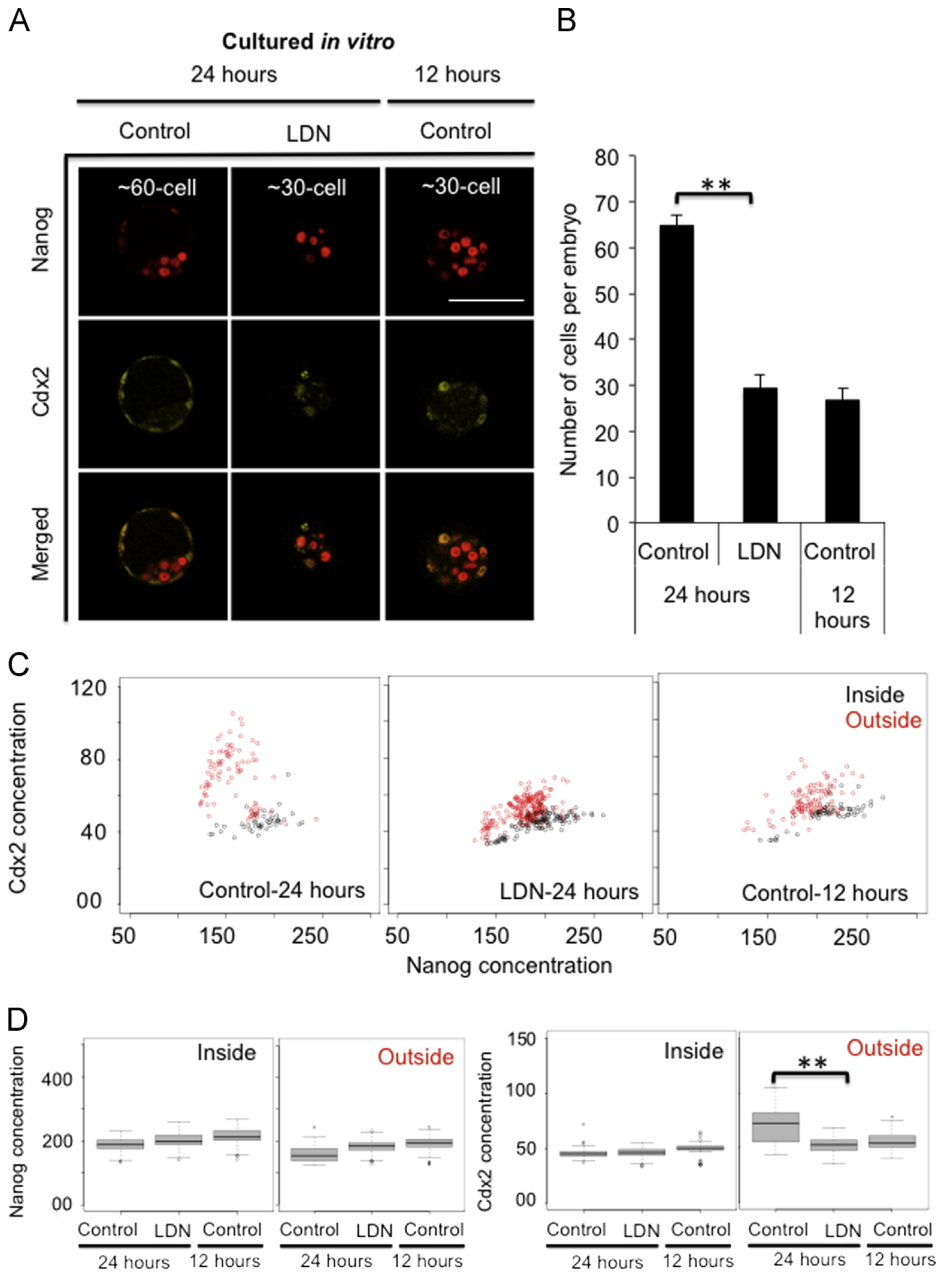

Fig. 6. BMP signaling inhibition delays blastocyst development. (A) Embryos isolated at E2.5 were cultured *in vitro* with and without LDN193189 for 24 h and stained for Nanog and Cdx2 (top and middle). Cell number-matched control embryos cultured for 12 h (right). (B) The average total cell number of LDN193189 treated embryos (~30 cells per embryo, $n=12$) is significantly reduced when compared to the embryos cultured for 24 h (~60 cells per embryo, $n=4$), but is comparable to the 12 h cultured embryos (~30 cells per embryo, $n=8$). (C and D) Scatter plots and box- whisker plots of Nanog and Cdx2 concentrations in individual blastomeres (inside black and outside red) blastomeres. Blastomeres of LDN193189 treated embryos displayed a significant decrease in Cdx2 concentration (control mean of 72.4 and LDN193189 mean of 52.8, $p<0.001$). Scale = 100 μm, SEM is reported.

cells do not respond to endogenous levels of BMPs present in serum under *in vitro* culture condition. We postulate this is because BRE-gal mES cells respond to moderate levels of BMP signaling and the amount of BMP signaling present in *in vitro* culture condition is insufficient to provide strong β-gal activity. Alternatively, exposure to serum stimulates pathways that inhibit BMP signaling intracellularly. Consistent with this notion, weak β-gal activity was observed when BRE-gal mES cells were incubated in X-gal substrate for a longer period of time. Additionally, in the monolayer of BRE-gal mES cells, we observed patches of cells showing stronger β-gal activity (Fig. S2B, serum control). These X-gal positive ES cells may represent ES cells responding to high concentrations of local BMP signaling influenced by neighboring cells. In that light, it is interesting to note that X-gal staining of mouse morula stage embryos is significantly stronger than that of *in vitro* cultured BRE-gal ES cells, suggesting that the endogenous level of BMP activity present in mouse morula stage and blastocysts is relatively high.

The available expression data for BMP signaling components during mammalian development suggests that qualitatively different BMP signaling may occur across preimplantation stages. Both Tang et al. (2010) and Wicher et al. (personal communication) observed that the inner and outer cells of morula-stage mouse embryos display differential expression of BMP ligands and receptors. BMP6 and BMP7 are expressed early and their expression declines quickly after fertilization, while BMP4 expression becomes enriched in the ICM of developing blastocysts (Coucouvanis and Martin, 1999; Fig. S1). BMP receptor 1a (Bmpr1a/ALK3) and 1b (Bmpr1b/ALK6)

are differentially expressed zygotically, whereas the type II receptor *Bmpr2* is expressed exclusively in outside cells (Wicher et al., personal communication). BMP ligands are also known to bind to other ALK family receptors to activate Smad1/5/8 signaling (Roelen et al., 1997; Maserbourg et al., 2005). Based on these expression data, we hypothesize that BMP signaling inputs for ICM and TE cells are mediated via utilization of different BMP ligands and receptors, and thus transcriptional machinery. This model is consistent with our observations indicating the presence of BMP signaling in both ICM and TE cells, but displaying differential transcriptional response toward BRE-reporter gene in ICM and TE cells (Fig. 1). The differential response of ICM and TE cells toward BMP signaling is likely to depend on the utilization of different transcription factors present in ICM and TE cells, which are expected to partner with Smad1/4 differentially.

These instances of qualitatively different BMP signaling during blastocyst formation may not be apparent by examination of p-Smad1 immunostaining, as p-Smad1 staining represents a general readout of overall canonical BMP signaling activity and this approach is unable to distinguish different pathways of BMP signaling. Specifically, different sets of targets can be modulated at different developmental time in different tissues, dependent on the availability of different Smad partners and receptors. It will be important to better define the spatio-temporal expression patterns of various BMP signaling components within the embryo in order to elucidate the roles these components play during preimplantation stage mouse development, a crucial step in the reconciliation and incorporation of BMP signaling pathway data into the current gene regulatory network addressing blastocyst formation in the mouse.

Experimental procedures

Detailed description of materials and methods are described in supplemental information

Embryo acquisition and in vitro culture

Preimplantation stage mouse embryos were collected at desired embryonic day by flushing uterine horns or oviducts with Dulbecco's Modified Eagle Medium (DMEM) with Hepes (10 mM, pH 7.3) media. Embryos were rinsed in flushing and holding media three times before culturing *in vitro* in micro-droplets containing KSOMaa (Life Technologies) and solvent control-DMSO (Sigma Aldrich), which were layered with light mineral oil (Sigma Aldrich) When necessary, LDN193189 (Stemgent) or Noggin (R&D Systems) were included in KSOMaa micro-droplets. Mouse embryos were staged according Gardner (1997).

ES cell culturing, cell transfection, and Western blot

Mouse E14Tg2a ES cells were maintained in GMEM medium (Sigma Aldrich) with 10% FBS (Hyclone) DNBR-HA and pCMV-β-gal constructs were transfected into ES cells using Lipoectamine2000 (Invitrogen). For Western blot analysis, cells were homogenized in RIPA buffer and subjected to gel electrophoresis. Primary antibodies (see Table S2) were anti-p-Smad1 (1:500, Millipore), anti-Smad (1:200, Santa Cruz Biotechnology), anti-HA (1:200, Santa Cruz biotechnology), or anti-Tubulin (1:10,000, Life Technologies).

Quantitative polymerase chain reaction (qPCR)

RNAs were isolated after treatment of E14Tg2a mES cells with hBMP4 (R&D Systems) or LDN193189 (Stemgent) using Trizol (Life Technologies). Reverse transcription was performed using MMLV Reverse Transcriptase according to manufacturer's guideline. Quantitative PCR reactions were performed using Sybr-Green (Roche) and the primers listed in Supplemental Materials and methods.

X-gal and immunofluorescence staining

For X-gal staining, E14Tg2a cells were rinsed in pre-warmed PBS, fixed in 0.05% glutaraldehyde at room temperature for 15 minutes and incubated in X-gal (10 μg/ml) at 37 °C. Preimplantation stage mouse embryos were fixed in 4% paraformaldehyde, washed, and incubated with X-gal overnight.

For immunostaining, E14Tg2a mES cells were fixed with 3.7% formaldehyde in 1X PBS, rinsed with 1X PBS, and incubated in permeabilization buffer (0.24% Triton-X100) for 15 min at room temperature. After pre-incubation with blocking solution, the cells were incubated with indicated primary antibodies, anti-p-Smad1/5/8 (1:100, Millipore) or anti-SMAD1/5/8 (1:200, Santa Cruz Biotechnology) overnight. Secondary antibodies were goat anti-rabbit-Alexa555 (1:200, Life Technologies) and donkey anti-mouse Cruz647 (1:200, Santa Cruz Biotechnology). Preimplantation stage mouse embryos were rinsed in Acid Tyrode's solution, (Sigma Aldrich), followed by a 30 min fixation with 3.7% formaldehyde. Primary antibodies used (see Table S2) were anti-p-Smad1/5/8 (1:50 & 1:100, Millipore), anti-Smad1/5/8 (1:200, Santa Cruz Biotechnology), anti-Cdx2 (1:200, BioGenex), and anti-Nanog (1:200, Cosmo Bio USA). Additionally, E14Tg2a mES cells and embryos were stained with Hoechst (2 μg/ml, Sigma Aldrich) and Phalloidin-488 (1:40 dilution, Life Technologies) for nuclear and F-actin staining, respectively. Embryos were placed on a glass slide coated with a 1% agarose pad and compressed to a 3:1 aspect ratio. All confocal images were acquired using a 20 × 0.8 NA (mES cells) and 63 × 1.4 NA (embryos) objective, on an Axioobserver Z1 Zeiss 780 confocal microscope with Zen2009 software. Z-stack images were acquired at 0.3 μm intervals.

Live imaging

Live imaging of H2BeGFP embryos was performed as previously described (Kurotaki et al., 2007). A Leica microscope equipped with Hamamatsu 1K EM-CCD was used.

Fluorescence quantification via image segmentation

We generated segmentation masks for individual nuclei in fluorescence microscopy images of the early mouse embryo. First, we manually annotated cell centers based on DNA images. Cell labels (such as inside/outside/ICM/trophectoderm) were manually assigned at this stage. Second, we preprocessed the DNA image for segmentation by normalizing, blurring, and inverting the image. Third, we generated segmentation masks by running active contours initialized from the annotated cell centers (De Solorzano et al., 2001). Expansion of active contour boundaries was constrained by areas of low intensity in the original DNA image and by collisions with neighbors. A sample segmentation is given in Fig. 2A. Lastly, we quantified p-Smad1/Nanog/Cdx2 concentration by computing the average pixel intensity in individual nuclear segmentation masks.

Embryos in each experiment were imaged in the same session; this enabled direct comparison of fluorescence contents across embryos in the same experiment. In order to verify accuracy of our segmentation procedure, we compared fluorescence contents derived from our procedure *versus* manual segmentations (generated using the Fiji Segmentation Editor; Schindelin et al., 2012) and found close agreement (R^2 of 0.98–0.94, Fig. S3A). In order to minimize the impact of fluorescence attenuation along the *z*-axis of the image, we only used "top layer" nuclei in subsequent analysis (nuclei whose projection to the top of the stack was at least 10% free of overlap with nuclei closer to the top of the stack): fluorescence from "top layer" nuclei is minimally attenuated since there is a minimal amount of tissue to traverse. In addition, mitotic and polar body cells were annotated based on DNA morphology and excluded from subsequent analysis.

Above, we assay fluorescence levels via concentration (*i.e.*, average pixel intensity). An alternative method of assaying fluorescence levels is to compute total content (*i.e.*, summed pixel intensities). In 64-cell stage embryos, significant differences in p-Smad1 levels exist in ICM/TE cells when measured via total content. However, these differences are relatively small (7%) compared to results derived p-Smad1 concentrations (27%, Table S1). We speculate that nuclear p-Smad1 concentration may be a better readout of BMP signaling than total nuclear p-Smad1 content.

Data analysis

All *p*-values were computed using Student's *t*-test (R studio, Matlab). Images were visualized using ImageJ (NIH http://imagej.nih.gov/ij/).

Dominant negative BMP receptor 1a expression construct and DNA microinjections

Bmpr1aCA-pCIG pRosa26-DEST (gift from Edwin Monuki, Lim et al., 2004) was used to generate DNA encoding a dominant negative BMP receptor (DNBR-HA), which was sub-cloned into pCS2+HA. Subsequently, the DNBR-HA was subcloned into pCMV-β (MacGregor and Caskey, 1989). The human cytomegalovirus (CMV) immediate early promoter (IEP), a splice acceptor–donor region, precedes the DNBR-HA sequence. Lastly, an oligo adapter with the P2A sequence was subcloned into pCS2-mCherry. The P2A-mCherry fragment was cloned into the pCMV-DNBR-HA vector to complete the construct that expresses both DNBR-HA and mCherry under transcriptional control of the CMV IEP. C57BL/6NTac 3-week old females were superovulated and embryos were harvested at the 2-cell stage (embryonic day e1.5) (Nagy et al., 2003). DNA fragments were gel purified, passed through a 0.22 μm filter and injected into a single blastomere of 2-cell stage embryos at a final concentration of 1.5 ng/μl total DNA. After microinjection, embryos were washed four times and transferred in KSOMaa media and incubated at 37 °C under hypoxic conditions (90% N_2, 5% CO_2, 5% O_2) in 25 μl microdrops of pre-equilibrated media in a Planer BT37 (Planer PLC, Sunbury-On-Thames, England) until the required developmental stage was reached. Images were collected using Olympus DP70.

Acknowledgements

We thank the Transgenic Mouse Facility at University of California, Irvine for blastomere injections, Dr. Amanda Cinquin for advice on confocal microscopy and immunostaining, Dr. Magdalena Zernicka-Goetz for sharing unpublished data, and Dr. Ed Monuki for p-Smad1 antibody and pCIG-DNBR. We thank Dr. Ira Blitz for his intellectual and editorial input, Dr. Hiroshi Sasaki for discussion, and Ms. Krishna Patel for immunohistology and genotyping. This work was funded by NIH (R01-HD056219 to KC and R01-GM102635 to OC, F31-HD074409 and R25GM055246 for NM, and T32-HD060555 and T15-LM007443 for MC). Additionally, research reported in this publication was supported by the National Cancer Institute of the National Institutes of Health under Award Number P30CA062203. The content is solely the responsibility of the authors and does not necessarily represent the official views of the National Institutes of Health.

Appendix A. Supporting information

Supplementary data associated with this article can be found in the online version at http://dx.doi.org/10.1016/j.ydbio.2014.10.001.

References

Alexander, C., Zuniga, E., Blitz, I.L., Wada, N., LePabic, P., Javidan, Y., Zhang, T., Cho, K.W.Y., Crump, J.G., Schilling, T., 2011. Combinatorial roles for Bmps and Endothelin1 in patterning the dorsal–ventral axis of the craniofacial skeleton. Development 138, 5135–5146.

Arnold, S.J., Maretto, S., Islam, A., Bikoff, E.K., Robertson, E.J., 2006. Dose-dependent Smad1, Smad5, and Smad8 signaling in the early mouse embryo. Dev. Biol. 296 (1), 104–118.

Avilion, A.A., Nicolis, S.K., Pevny, L.H., Perez, L., Vivian, N., Lovell-Badge, R., 2003. Multipotent cell lineages in early mouse development depend on SOX2 function. Genes Dev. 17, 126–140.

Beppu, H., Kawabata, M., Hamamoto, T., Chytil, A., Minowa, O., Noda, T., Miyazono, K., 2000. BMP Type II receptor is required for gastrulation and early development of mouse embryos. Dev. Biol. 221, 249–258.

Chambers, I., Colby, D., Robertson, M., Nichols, J., Lee, S., Tweedie, S., Smith, A., 2003. Functional expression cloning of Nanog, a pluripotency sustaining factor in embryonic stem cells. Cell 113, 643–655.

Chu, G.C., Dunn, N.R., Anderson, D.C., Oxburgh, L., Robertson, E.J., 2004. Differential requirements for Smad4 in TGFbeta-dependent patterning of the early mouse embryo. Development 131 (15), 3501–3512.

Ciemerych, M., Sicinski, P., 2005. Cell cycle in mouse development. Oncogene 24, 2877–2898.

Copp, A.J., 1978. Interaction between inner cell mass and trophectoderm of mouse blastocyst. I. A study of cellular proliferation. J. Embryol. Exper. Morpho 48, 109–125.

Coucouvanis, E., Martin, G.R., 1999. BMP signaling plays a role in visceral endoderm differentiation and cavitation in the early mouse embryo. Development 126, 535–546.

Cuny, G.D., Yu, P.B., Laha, J.K., Xing, X., Liu, J.F., Lai, C.S., Deng, D.Y., Sachidanandan, C., Bloch, K.D., Peterson, R.T., 2008. Structure-activity relationship study of bone morphogenetic protein (BMP) signaling inhibitors. Bioorg. Med. Chem. Lett. 18, 4388–4392.

Derynck, R., Zhang, Y.E., 2003. Smad-dependent and Smad-independent pathways in TGF-beta family signaling. Nat. 425, 577–584.

De Solorzano, C.O., Malladi, R., Lelièvre, S.A., Lockett, S.J., 2001. Segmentation of nuclei and cells using membrane related protein markers. J. Microsc. 201 (Pt 3), 404–415.

Dietrich, J.E., Hiiragi, T., 2007. Stochastic patterning in the mouse pre-implantation embryo. Development 134, 4219–4231.

Doan, L., Javier, A., Cho, K.W.Y., Monuki, E., 2012. A Bmp reporter with ultrasensitive characteristics reveals that high Bmp signaling is not required for cortical hem fate. PLoS One 7 (9), e44009.

Eom, D.S., Amarnath, S., Fogel, J.L., Agarwala, S., 2011. Bone morphogenetic proteins regulate neural tube closure by interacting with the apicobasal polarity pathway. Development 138, 3179–3188.

Fuentealba, L.C., Eivers, E., Ikeda, A., Hurtado, C., Kuroda, H., Pera, E.M., De Robertis, E.M., 2007. Integrating patterning signals: wnt/gsk3 regulates the duration of the BMP/Smad1 signal. Cell 131 (5), 980–993.

Gardner, R.L., 1997. The early blastocyst is bilaterally symmetrical and its axis of symmetry is aligned with the animal–vegetal axis of the zygote in the mouse. Development 124 (2), 289–301.

Gardner, R.L., Davies, T.J., 2002. Trophectoderm growth and bilateral symmetry of the blastocyst in the mouse. Hum. Reproduct. 17 (7), 1839–1845.

Guo, G., Huss, M., Tong, G.Q., Wang, C., Sun, L.L., Clarke, N.D., Robson, P., 2010. Resolution of cell fate decisions revealed by single-cell gene expression analysis from zygote to blastocyst. Dev. Cell 18, 675–688.

Hogg, K., Etherington, S.L., Young, J.M., McNeilly, A.S., Duncan, W.C., 2010. Inhibitor of differentiation (ID) genes are expressed in the steriodogenic cells of the ovine ovary and are differentially regulated by members of the transforming growth factor-b family. Endocrinology 151 (3), 1247–1256.

Hollnagel, A., Oehlmann, V., Heymer, J., Ruther, U., Nordheim, A., 1999. Id genes are direct targets of bone morphogenetic protein induction in embryonic stem cells. J. Biol. Chem. 274 (28), 19838–19845.

Javier, A., Doan, L., Luong, M., Reyes de Mochel, N.S., Blitz, I.L., Monuki, E., Cho, K.W.Y., 2012. Dynamically regulated expression patterns of BMP signaling using BRE-gal indicator mice. PLoS One 7, e42566.

Komatsu, Y., Kaartinen, V., Mishina, Y., 2011. Cell cycle arrest in node cells governs cilliogenesis at the node to break left-right symmetry. Development 138 (18), 3915–3920.

Kretzschmar, M., Doody, J., Massague, J., 1997. Opposing BMP and EGF signaling pathways converge on the TGF-beta family mediator Smad1. Nature 389 (6651), 618–622.

Kurotaki, Y., Hatta, K., Nakao, K., Nabeshima, Y., Fujimori, T., 2007. Blastocysts axis is specified independently of early cell lineage but aligns with the ZP shape. Science 316, 719–723.

Lim, Y., Cho, G., Minarcik, J., Golden, J., 2004. Altered BMP signaling disrupts chick diencephalic development. Mech. Dev. 122, 603–620.

MacGregor, G.R., Caskey, C.T., 1989. Construction of plasmids that express E. coli beta-galactosidase in mammalian cells. Nucleic. Acids Res. 17, 2365.

Macías-Silva, M., Hoodless, P.A., Tang, S.J., Buchwald, M., Wrana, J.L., 1998. Specific activation of Smad1 signaling pathways by the BMP7 type I receptor, ALK2. J. Biol. Chem. 273 (40), 25628–25636.

Maretto, S., Cordenonsi, M., Dupont, S., Braghetta, P., Broccoli, V., Hassan, A.B., Volpin, D., Bressan, G.M., Piccolo, S., 2003. Mapping Wnt/beta-catenin signaling

during mouse development and in colorectal tumors. Proc. Natl. Acad. Sci. U.S.A. 100, 3299–3304.
Martin, R.M., Leonhardt, H., Cardoso, M.C., 2005. DNA labeling in living cells. Cytomerty Part A 67A, 45–52.
Maserbourg, S., Snagkuhl, K., Luo, C.W., Sudo, S., Klein, C., Hsueh, A.J.W., 2005. Identification of receptors and signaling pathways for orphan bone morphogenetic protein/growth differentiation factor ligands based on genomic analysis. J. Biol. Chem. 280, 32122–32132.
Massari, M.E., Murre, C., 2000. Helix–loop–helix proteins: regulators of transcription in eukaryotic organisms. Mol. Cell Biol. 20, 429–440.
Mishina, Y., Suzuki, A., Ueno, N., Behringer, R.R., 1995. Bmpr encodes a type I bone morphogenetic protein receptor that is essential for gastrulation during mouse embryogenesis. Genes Dev. 9, 3027–3037.
Moustakas, A., Heldin, C.H., 2005. Non-Smad TGF-beta signals. J. Cell Sci. 118 (16), 3573–3584.
Murre, C., McCaw, P.S., Vaessin, H., Caudy, M., Jan, L.Y., Jan, Y.N., Cabrera, C.V., Buskin, J.N., Hauschka, S.D., Lassar, A.B., Weintraub, H., Baltimore, D., 1989. Interactions between heterologous helix–loop–helix proteins generate complexes that bind specifically to a common DNA sequence. Cell 58, 537–544.
Nagy, A., Gertsenstein, M., Vintersten, K., Behringer, R., 2003. Manipulating the Mouse Embryo. Cold Spring Harbor Press, New York (Cold Spring Harbor).
Natale, D.R., Paliga, A.J.M., Beier, F., D'Souza, S.J.A., Watson, A.J., 2004. 38 MAPK signaling during marine preimplantation development. Dev. Biol. 268, 76–88.
Nichols, J., Sevnik, B., Anastassiadis, K., Niwa, H., Klewe-Nebenius, D., Chambers, I., Scholer, H., Smith, A., 1998. Formation of pluripotent stem cells in the mammalian embryo depends on the POU transcription factor Oct4. Cell 95 (3), 37–91.
Nishioka, N., Yamamoto, S., Kiyonari, H., Sato, H., Sawada, A., Ota, M., Nakao, K., Sasaki, H., 2008. Tead4 is required for specification of trophectoderm in pre-implantation mouse embryos. Mech. Dev. 125 (3-4), 270–283.
Roelen, B.A.J., Goumans, M.J., Van Rooijen, M.A., Mummery, C.L., 1997. Differential expression of BMP receptors in early mouse development. Int. J. Dev. Biol. 41, 541–549.
Rossant, J., Tam, P.P.L., 2009. Blastocyst lineage formation, early embryonic asymmetries and axis patterning in the mouse. Development 136, 701–713.
Sapkota, G., Alarcon, C., Spagnoli, F.M., Brivanlou, A.H., Massague, J., 2007. Balancing BMP signaling through integrated inputs into the Smad1 linker. Mol. Cell 25, 441–454.
Schindelin, J., Arganda-Carreras, I., Frise, E., Kaying, V., Longair, M., Pietzsch, T., Preilbisch, S., Rueden, C., Saafeld, S., Schmid, B., Tinevez, J.Y., White, D.J., Hartenstein, V., Ellceiri, K., Tomancak, P., Cardona, A., 2012. Fiji: an open-source platform for biological image analysis. Nat. Methods 9, 676–682.
Smith, R., McLaren, A., 1977. Factors affecting the time of formation of the mouse blastocoel. J. Embryol. Exp. Morph. 41, 79–92.
Solloway, M.J., Robertson, E.J., 1999. Early embryonic lethality in Bmp5;Bmp7 double mutant mice suggests functional redundancy within the 60A subgroup. Development 126, 1753–1768.
Strumpf, D., Mao, C.A., Yamanaka, Y., Ralston, A., Chawengsaksophak, K., Beck, F., Rossant, J., 2005. Cdx2 is required for correct cell fate specification and differentiation of trophectoderm in the mouse blastocyst. Development 132, 2093–2102.
Takaku, K., Oshima, M., Miyoshi, H., Matsui, M., Seldin, M.F., Taketo, M.M., 1998. Intestinal tumorigenesis in compound mutant mice of both Dpc4 (Smad4) and Apc genes. Cell 92, 645–656.
Tang, F., Barbacioru, C., Bao, S., Lee, C., Nordman, E., Wang, X., Lao, K., Surani, A., 2010. Tracing the derivation of embryonic stem cells from the inner cell mass by single-cell RNA-Seq analysis. Cell Stem Cell 6, 468–478.
Vogt, J., Traynor, R., Sapkota, G.P., 2011. The specificities of small molecule inhibitors of the TGFß and BMP pathways. Cell Signal 23 (11), 1831–1842.
von Bubnoff, A., Peiffer, D., Blitz, A., HayataT., I.L., Ogata, S., Miyazono, K., Cho, K.W.Y., 2005. Phylogenetic footprinting and genome scanning identifies vertebrate BMP response elements and new target genes. Dev. Biol. 281, 210–226.
Wang, H., Dey, S.K., 2006. Roadmap to embryo implantation: clues from mouse models. Nat. Rev. Genet. 3, 185–199.
Westermarck, S.P., Li, T., Kallunki, J., Han, J., Kahari, V.M., 2001. P38 mitogen-activated protein kinase-dependent activation of protein phosphatases 1 and 2A inhibits MEK1 and MEK2 activity and collagenase 1 (MMP-1) gene expression. Mol. Cell Biol. 21 (7), 2373–2383.
White, E., 1996. Life, death, and the pursuit of apoptosis. Genes Dev. 10, 1–15.
Yagi, R., Kohn, M.J., Karavanova, I., Kaneko, K.J., Vullhorst, D., DePamphilis, M.L., Buonanno, A., 2007. Transcription factor TEAD4 specifies the trophectoderm lineage at the beginning of mammalian development. Development 134 (21), 3827–3836.
Yamaguchi, K., Shirakabe, K., Shibuya, H., Irie, K., Oishi, I., Ueno, N., Taniguchi, T., Nishida, E., Matsumoto, K., 1995. Identification of a member of the MAPKKK family as a potential mediator of TGF-beta signal transduction. Science 270 (5244), 2008–2011.
Yamaguchi, K., Nagai, S., Ninomiya-Tsuji, J., Nishita, M., Tamai, K., Irie, K., Ueno, N., Nishida, E., Shibuya, h., Matsumoto, K., 1999. XIAP, a cellular member of the inhibitor of apoptosis protein family, links the receptors of Table1-TAK1 in the BMP signaling pathway. EMBO J. 18 (1), 179–187.
Yao, L.C., Blitz, I.L., Peiffer, D.A., Phin, S., Wang, Y., Ogata, S., Cho, K.W.Y., Arora, K., Warrior, R., 2006. Transcription factors mediate a phylogenetically conserved nuclear response to BMP signaling. Development 133, 4025–4034.
Yi, S.E., Daluiski, A., Pederson, R., Rosen, V., Lyons, K.M., 2009. The type I BMP receptor BMPRIB is required for chondrogenesis in the mouse limb. Development 127 (3), 621–630.
Ying, Q.L., Nichols, J., Chambers, I., Smith, A., 2003. BMP induction of Id proteins suppresses differentiation and sustains embryonic stem cell self-renewal in collaboration with STAT3. Cell 115 (3), 281–292.
Yu, Y.B., Hong, C.C., Sachidanandan, C., Babitt, J.L., Deng, D.Y., Hoyng, S.A., Lin, H.Y., Bloch, K.D., Peterson, R.T., 2008. Dorsomorphin inhibits BMP signals required for embryogenesis and iron metabolism. Nat. Chem. Biol. 4, 33–41.
Zernicka-Goetz, M., Morris, S.A., Bruce, A.W., 2009. Making a firm decision: multifaceted regulation of cell fate in the early mouse embryo. Nat. Rev. Genet. 10, 467–477.
Ziomek, C.A., Johnson, M.H., Handyside, A.H., 1982. The developmental potential of mouse 16-cell blastomeres. J. Exp. Zool. 221, 345–355.

Figure S1

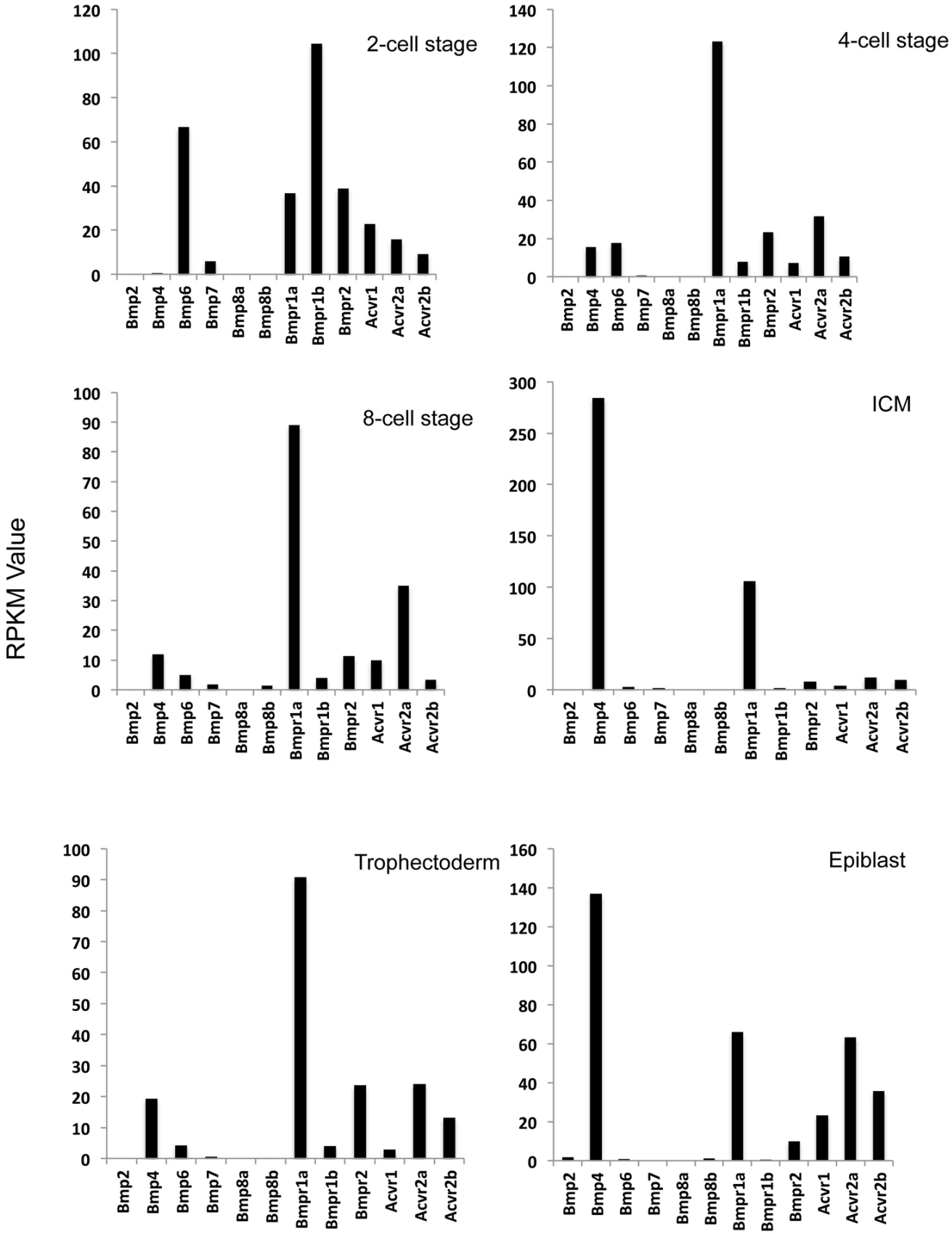
RPKM Value
2-cell stage
4-cell stage
8-cell stage
ICM
Trophectoderm
Epiblast
Bmp2
Bmp4
Bmp6
Bmp7
Bmp8a
Bmp8b
Bmpr1a
Bmpr1b
Bmpr2
Acvr1
Acvr2a
Acvr2b

Figure S2, related to figure 1

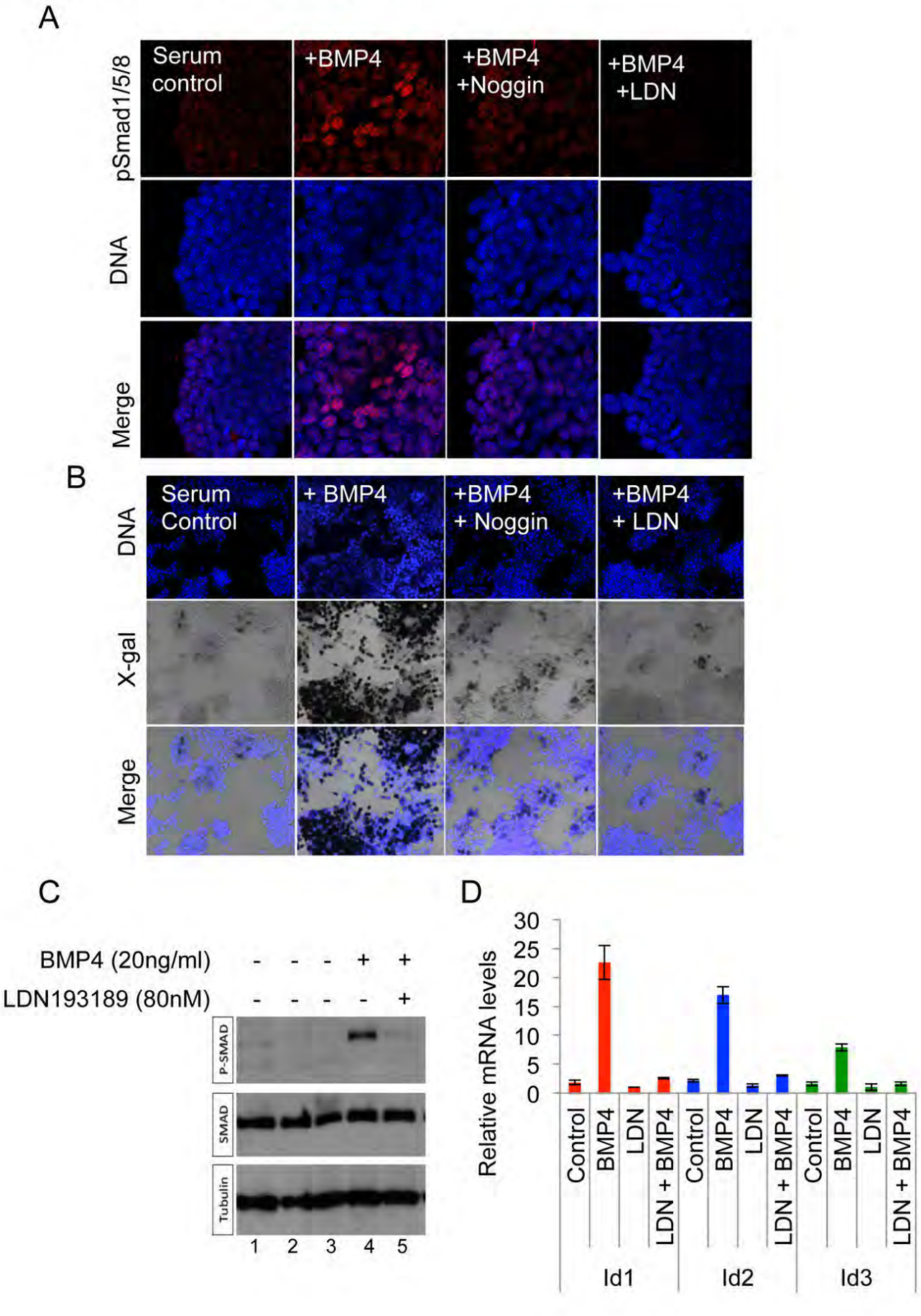

Figure S3 , related to figure 2

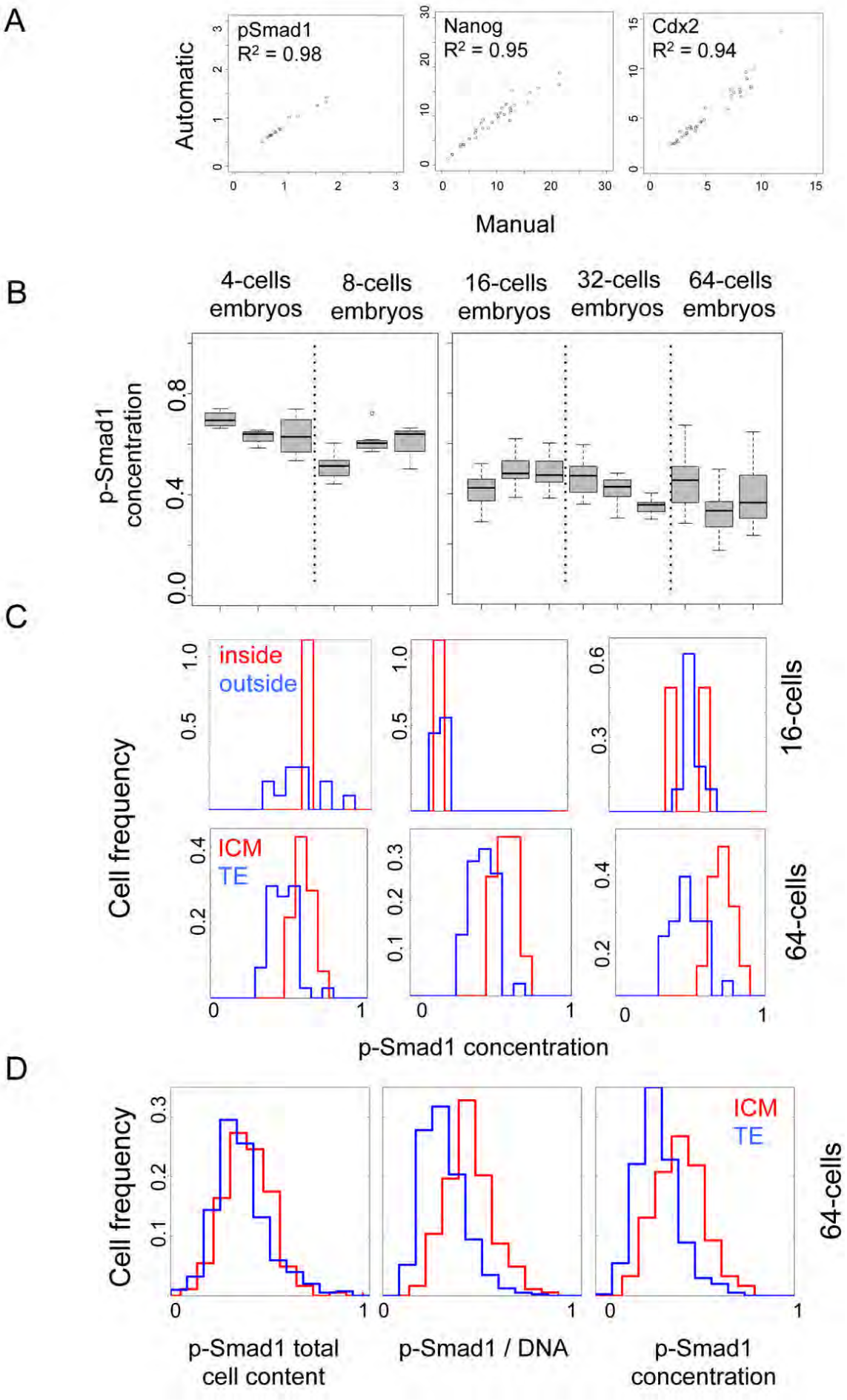

Figure S4, related to figure 3

A

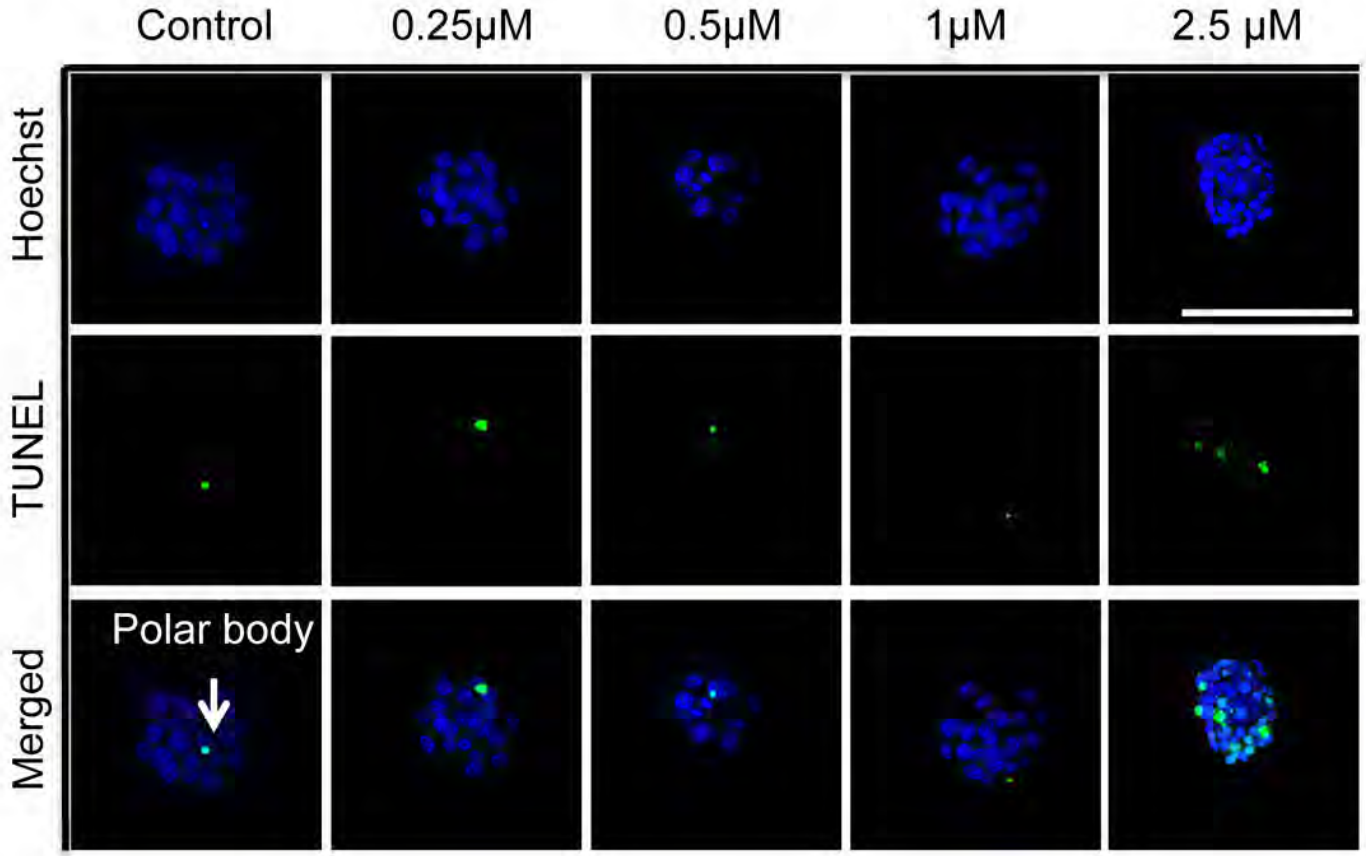

Figure S5, related to Figure 4

A

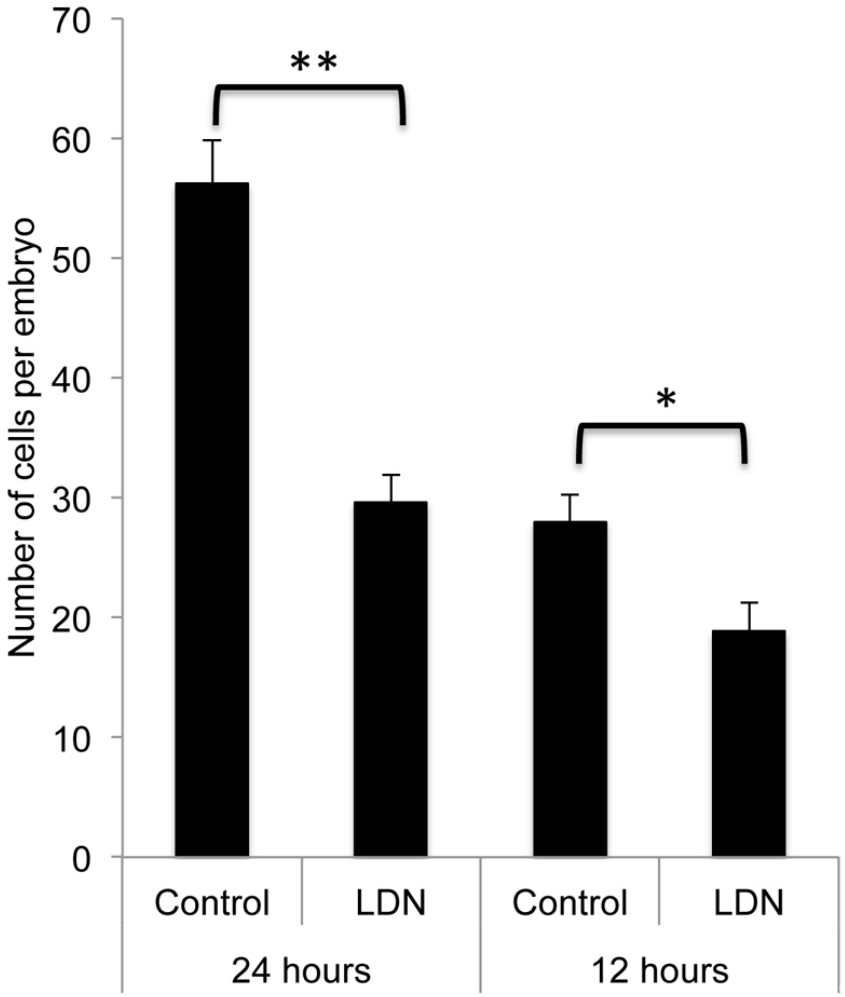

B

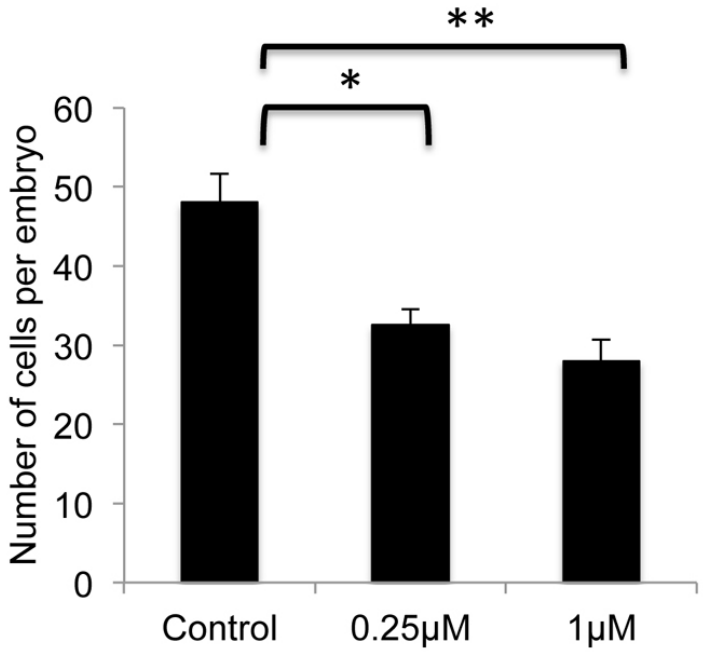

Figure S6, related to figure 5

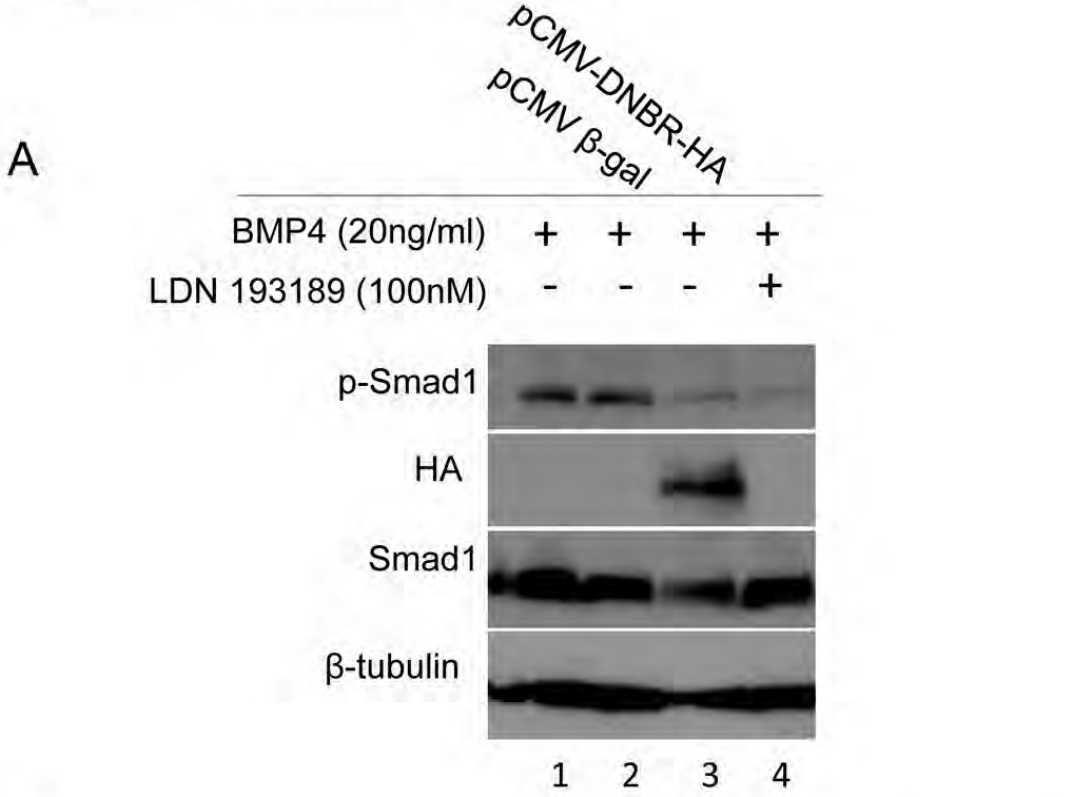

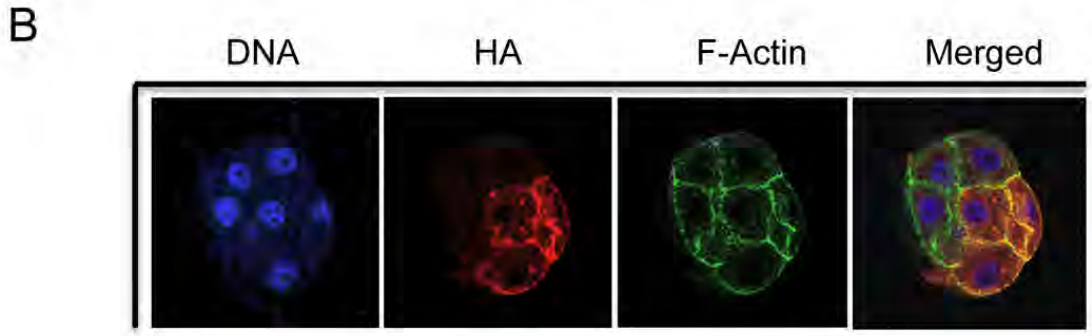

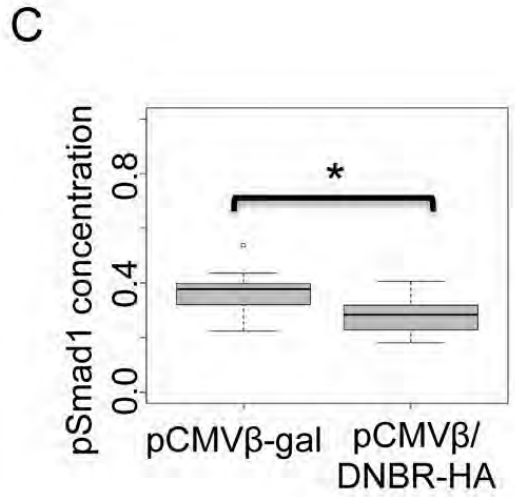

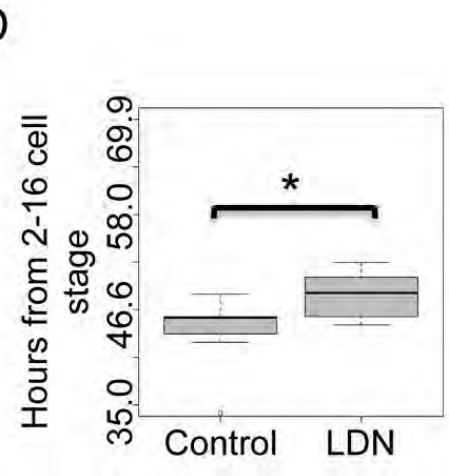

Supplemental Figure Legends

Figure S1: RPKM analysis of single cell RNA-seq data.

Varying amount of transcripts encoding the indicated BMP ligands and receptors are present in 2-cell, 4-cell, 8-cell stage embryos. ICM and trophectoderm cells of blastocysts express some common and different BMP ligands and receptors.

Figure S2: LDN specifically inhibits BMP signaling in mouse mES cells, related to Figure 1

A) Phosphorylated Smad1/5/8 is present in the nucleus following stimulation with BMP4 (20ng/ml) and significantly reduced when co-treated with BMP antagonists, Noggin (50ng/ml) or LDN193189 (80nM). DNA is in blue, pSmad1 in red. B) LDN193189 (80nM) and Noggin (50ng/ml) inhibit BRE-gal expression in mouse ES (mES) cells after BMP4 (20ng/ml) stimulation. C) Western blot of E14Tg2a mES cells treated with BMP4 (20ng/ml) in presence or absence of LDN193189 (80nM). Phosphorylated Smad1 (p-Smad1) is detected upon BMP4 stimulation (lane 4) and in the presence of LDN193189, Smad1 phosphorylation is inhibited (lane 5). D) qRT-PCR analysis of *Id* genes in mES cells cultured in the presence of BMP4 (BMP4 20ng/ml), LDN193189 (80nM), or both.

Figure S3: Fluorescence intensity quantification of p-Smad1, related to Figure 2

A) Correlations of pSmad1 (R^2=0.98), Nanog (R^2=0.95), and Cdx2 (R^2=0.94) concentrations between automatic (y-axis) and manual (x-axis) segmentations. B) pSmad-1 concentration in three individual 4- and 8-cell stage embryos (left panel) and embryos at 16-, 32- and 64- cell stage (right panel). C) Distribution of nuclear pSmad1 concentrations in 3 16-cell embryos and 3 64-cell embryos (inside and ICM cells in red and outside and TE in blue). D) pSmad1 total nuclear content (computed as the sum of pixel intensities), pSmad1 content normalized by DNA content, and pSmad1 concentration in cells from 13 aggregated 64-cell embryos (ICM cells shown in red and TE cells in blue). A Student's *t*-test was used to test whether different methods yielded significantly-different results (refer to supplement Table S1). Y-axis represents relative fluorescence from low to high (0 to 1).

Figure S4: Effects of BMP signaling inhibition on apoptosis, related to Figure 3

A) TUNEL assay on embryos treated with LDN193189 for 24 hours. No TUNEL positive cell is found in embryos treated with 0.25μM (n = 6), 0.5μM (n=12), 1μM (n=16) of LDN139189. At 2.5 μM LDN139189 (n=5), TUNEL-positive cells are detected. Note polar bodies are TUNEL-positive in control and other LDN193189 treated embryos. DNA in blue, TUNEL positive cells in green. Scale bar = 100μm.

Figure S5: Reduced cell number in embryos cultured in LDN193189 for 12 hours, related to Figure 4

A) Total cell number is reduced in embryos cultured with LDN193189 for 12 hours (LDN, n=14, 18.8±2.4 cells, control, n=10, 28±2.2 cells) and 24 hours (LDN, n=6, 29.6±2.2 cells, control, n=25, 56.2±3.5 cells). B) Average numbers of cells per embryo decreases in the presence of 0.25μM LDN193189 (32.5±2.0 cells, n= 8). *p<0.05 and **p<0.001. SEM is reported and a Student's *t*-test was used to determine significance.

Figure S6: Effects of pCMV-DNBR-HA and LDN193189 in mouse mES cells and embryos, related to Figure 5

A) Western blot demonstrating an increase of phosphorylated Smad1 after BMP4 (20ng/ml) stimulation. Smad1 phosphorylation is inhibited after DNBR-HA expression in E14Tg2a mES cells. B) HA-tagged DNBR is detected on the membrane of cells in 8-cell stage embryo derived from the blastomere injected at the 2-cell stage. C) pSmad1 concentration decreases in pCMVβ/DNBR-HA (mean 0.27, n= 10) when compared to injected control pCMVβ (mean of 0.35, n=6, p<0.001). D) Increase in the number of hours embryos cultured in LDN193189 took to reach the 16-cell stage from 2-cell stage (control 44 hours, (n=16), LDN 48 hours, (n=17)). *p<0.05 and **p<0.001. SEM is reported and a Student's t -test was used to determine significance.

Table S1, Analysis of pSmad1 nuclear content, related to figure S3D

Figure -Data	**Total content**	**Normalized by DNA**	**Normalized by Volume**
Figure 2D 16-cell stage	Not significant Inside (mean 0.35) vs outside (mean 0.39) p>0.05 11% difference	Not significant Inside (mean 0.39) vs outside (mean 0.42) p>0.05 8% difference	Not significant Inside (mean 0.44) vs outside (mean 0.48) p>0.05 9% difference
Figure 2D 32-cell stage	Significant ICM (mean 0.32) vs TE (mean 0.36) P<0.05 12% difference	Not significant ICM (mean 0.40) vs TE (mean 0.43) P>0.05 7% difference	Not significant ICM (mean 0.49) vs TE (mean 0.47) p>0.05 4% difference
Figure 2D 64-cell stage	Significant ICM (mean 0.30) vs TE (mean 0.28) P<0.05 7% difference	Significant ICM (mean 0.41) vs TE (mean 0.29) p<0.001 30% difference	Significant ICM (mean 0.52) vs TE (mean 0.38) p<0.001 27% difference

Table S2, Antibodies used for this study

Antibody	Dilution used	Supplier	Catalog #	Lot #
Rabbit anti-pSmad1/5/8	1:50, 1;100, 1:500	Millipore	AB3848	2390361
Rabbit anti-Smad1/5/8 (N-18)-R	1:200	Santa Cruz Biotechnology Inc.	SC-6031_R	A1613
Rabbit anti-Oct3/4 (C-10)	1:250	Santa Cruz Biotechnology Inc.	SC-5279	Not available
Rabbit anti-nanog	1:200	Cosmo Bio Co.	RCAB0002P-F	20100713
Mouse Anti-Cdx2	1:200	BioGenex	MU392A-UC	MU392A0114X
Goat anti-Sox17	1:200	R&D	AF1924	KGA0613041
Rabbit anti-HA (Y-110	1:200	Santa Cruz Biotechnology Inc.	SC-805	A1205
Mouse anti-Tubulin	1:10,000	Life Technologies	T5168-2ml	051M4771
Goat anti-rabbit (Alexa-555)	1:200	Life Technologies	A21428	1511349
Donkey anti-rabbit (Alexa-555)	1:200	Life Technologies	A31572	1249018
Goat anti- mouse IgG-CFL647	1:200	Santa Cruz Biotechnology Inc.	SC-362287	D3013
Donkey anti- goat IgG-CFL647	1:200	Santa Cruz Biotechnology Inc.	SC-362285	B1313

Table S1 Analysis of pSmad1 nuclear content, related to Figure S3D

Table presenting pSmad1 total nuclear content (computed as the sum of pixel intensities), pSmad1 content normalized by DNA content, and pSmad1 concentration for data on Figure 2c (16-, 32-, and 64-cell stage embryos).

Table S2 Antibodies used for this study

Table of antibodies used for this study which includes, dilutions used, supplier, catalog #, and lot # information.

Supplemental Experimental Procedures

Embryo acquisition

Three-week old CD1 females (Charles River) were superovulated using pregnant mare serum (PMSG, Sigma Aldrich, catalog #G-4877, 2000IU/vial) followed ~ 45 hours later by human chorionic gonadotropin (hCG, Sigma Aldrich, catalog #C-1063, 2500IU/vial). All females received 5 IU doses of each hormone intraperitoneally. After hCG (Sigma Aldrich, catalog #C-1063, 2500IU/vial) injections, mating were set up. Females were checked the following morning for mating plugs, at which they were considered e0.5 if a vaginal plug was present. Embryos were collected at desired embryonic day by flushing uterine horns or oviducts with Dulbecco's Modified Eagle Medium (DMEM, Life Technologies, catalog #11965-092) with Hepes (10mM) media (Life Technologies, catalog #15630-106).

In vitro culture

Embryos were rinsed three times with DMEM (Life Technologies, catalog #11965-092) plus Hepes (Life Technologies, catalog #15630-106) and then prepared for *in vitro* culture in 35 µl microdroplets of KSOMaa (Life Technologies, catalog #MR-121-D*)* covered with a layer of light mineral oil (Sigma Aldrich, catalog #*M5310-1L*). The microdroplets were equilibrated at 37°C with 5% CO_2 for 1 hour prior to addition of embryos. All dissected embryos were imaged using

Olympus DP70. Embryos were incubated for 24 hours at 37°C, 5% CO_2 in a humidified Sanyo incubator (Sanyo Scientific).

mES cell culture

E14Tg2a mouse ES cells were cultured on 0.1% gelatin-coated plates containing GMEM medium (Sigma Aldrich, #G5153) with 10% FBS (Hyclone, catalog #SH30071.03), 0.1mM NEAA, 1mM Sodium Pyruvate, 1000U/ml LIF (Millipore, catalog #ESG1107), and 0.1mM 2-Mercaptoethanol. Cells were maintained at 37°C, 5% CO_2, and split using 0.25% trypsin (Life Technologies, catalog #15400-054).

mES cell transfection

pCMV-DNBR-HA and pCMV-β vectors were transfected into E14Tg2a mES cells using Lipofectamine2000 (Invitrogen, catalog #11668027) according to manufacture's protocol. Cells were collected for immunofluorescence or western blot analysis after 48 hrs post-transfection.

BMP signaling inhibition assay

LDN193189 (Stemgent, catalog #04-0074, lot#1861) was diluted in KSOMaa to a final concentration of 2.5μM, 1μM, 0.5μM, or 0.25μM from a 10mM stock (dissolved in DMSO, Sigma Aldrich, catalog #D2650). Embryos were placed in LDN193189/KSOMaa or Noggin/KSOMaa (R&D Sysems, catalog #1967-NG, lot#ETY08) microdroplets that had been pre-equilibrated for at least 1 hour.

Noggin (R&D Sysems, catalog #1967-NG, lot#ETY08) was dissolved in 1X PBS for final concentration of (50µg/ml, 10µg/ml, and 1µg/ml). Control embryos were similarly placed in microdroplets containing DMSO (Sigma Aldrich, catalog #D2650) solvent.

Immunofluorescence

mES cells: Cells were washed with 1X PBS (3x times), fixed with 3.7% formaldehyde for 15 minutes at room temperature (RT), rinsed with 1X PBS, and set in permeabilization buffer (0.25% Triton-X100 , Sigma Aldrich, catalog #107110934) for 15 minutes at RT. The cells were then blocked for 1 hour, and incubated in solution containing primary antibodies at 4°C overnight. Antibodies used were anti-pSMAD1,5,8 (1:100), anti-SMAD1,5 (1:200), and rabbit *anti*-Oct4 (1:250). After incubation, cells were rinsed with 1x PBS-Tween-20 (Fisher, catalog #EC-500-018-3) (0.1%) (1xPBS-T) then incubated with goat anti-rabbit-Alexa555 (1:200, Life Technologies) for 1 hour at room temperature. Additionally, cells were stained with Hoechst (2µg/ml, Sigma Aldrich, catalog #H21486) and Phalloidin-488 at 1:40 dilution (Life Technologies, catalog #A12379, 300U) for the nucleus and F-actin staining, respectively. All images were taken using Zeiss 780 confocal with 20x 0.8 NA objective with Zen2009 software.

Mouse embryos: Embryos were treated in Acid Tyrode solution for two minutes, rinsed in DMEM (Life Technologies, catalog #11965-092) plus Hepes (Life Technologies, catalog #15630-106), followed by a 30 minutes fixation with 3.7%

formaldehyde in 0.95X PBS on ice. Embryos were rinsed in 0.95X PBS and permeabilized for 15 minutes (0.2% TritonX-100 in 0.95X PBS) (Sigma Aldrich, catalog #107110934) before blocking for 1 hour at room temperature (0.2% BSA (Affymetrix, catalog #10868, lot#4135579), 0.2% TritonX-100, 2% goat, or donkey serum, in 0,95X PBS). All primary antibody incubations were performed at 4°C. Primary antibodies (see Table S2) were used at the following dilutions: anti-pSmad1,5,8 (1:50), anti-Smad1,5,8 (1:200), anti-Oct4 (1:250), anti-Sox17 (1:200), anti-Cdx2 (1:200), and anti-Nanog (1:200). Additionally, embryos were stained with Hoechst (2µg/ml, Life Technologies, catalog #H21486) and Phalloidin-488 (1:40 dilution, Life Technologies, catalog #A12379, 300U). All embryo images were acquired using a Zeiss 780 confocal microscope on a Zeiss AxioImager Z1 stand using a 63x, 1.4NA objective with Zen2009 software. Z-stack images were acquired at 0.3µm intervals for high-resolution 3D rendering.

Western Blotting

Mouse ES cells were collected in RIPA buffer (150mM NaCl, 50mM Tris-HCl pH 8.0, 1% NP40, 0.5% sodium deoxycholate, 0.1% SDS, 25mM β-glycerophosphate, 100nM NaF, and 1mM Na_3VO_4) and 15µg of protein lysates were electrophoresed through a 12% PAGE-SDS gel. Primary antibodies (see Table S2) used were: anti-p-Smad1 (1:500), anti-Smad (1:200), anti-HA (1:200), anti-β-tubulin (1:10,000). ECL kit (GE Healthcare, catalog #RPN2232) was used for visualization.

X-gal stain

Embryos collected at the desired embryonic stages were fixed in 4% paraformaldehyde (PFA) in 1X PBS for 30 minutes on ice. Before incubating embryos overnight with X-gal (10µg/ml) in X-gal stain solution butter (2mM $MgCl_2$, 5mM K ferrocyanide, 5mM K ferricyanide in 1X PBS) at 37°C, embryos were rinsed with Wash A (2mM $MgCl_2$ and 5mM EGTA in 1X PBS), then in Wash B (2mM $MgCl_2$, 0.01% sodium deoxycholate and 0.02% Nonidet P-40 1X PBS). ES cells were fixed in 0.05% glutaraldehyde solution and incubated in X-gal solution overnight 37°C. DNA of embryos and ES cells was stained with Hoechst (Life Technologies, catalog #H21486).

Quantitative Polymerase Chain Reaction (qPCR)

RNA was isolated after treatment of mES cells with 20ng/ml hBMP4 (R&D Systems, catalog #314-BP) or 80nM LDN193189 (Stemgent, Stemgent, catalog #04-0074, lot#1861) using Trizol (Life Technologies, catalog #15596-026). Reverse transcription was performed using MMLV Reverse Transcriptase (Invitrogen, catalog #28025-013) according to manufacture's guideline. Quantitative PCR was performed using SYBR Green (Roche, catalog #04-707-516-001).

Dominant negative BMP receptor 1a (DNBR) construct

To generate an epitope tagged DNBR, we used the Bmpr1aCA-pCIG pRosa26-DEST construct (gift from Dr. Edwin Monuki, UCI) to PCR amplify the DNBR

fragment containing ClaI (New England Bio Labs, catalog #R0197S) and NcoI ClaI (New England Bio Labs, catalog #R0193S) restriction sites at the 5'and 3' ends, respectively. The amplicons were sub-cloned into pCS2+HA, generating epitope tagged pCS2^{+}-DNBR-HA. An epitope tagged DNBR-HA fragment was subcloned into the HindIII (New England Bio Labs, catalog #R0104S) and HpaI (New England Bio Labs, catalog #R0105S) digested sites of pCMV-β after removing the LacZ gene. The resulting DNBR-HA gene resides downstream of the CMV immediate early promoter linked to splice acceptor/donor region. Primers for PCR amplification and sequencing are listed below.

DNA microinjections

All animal experimentation was conducted in accordance with federal guidelines for animal welfare with the studies being approved by the UCI Institutional Animal Care and Use Committee. UCI's Transgenic Mouse Facility (TMF) conducted all microinjection of mouse pre-implantation embryos. Briefly, C57BL/6NTac 3-week old females were superovulated using 5 IU of PMSG (Sigma Aldrich, catalog #G-4877, 2000IU/vial) followed ~ 45 hours later by 5 IU of hCG (Sigma Aldrich, catalog #C-1063, 2500IU/vial) and mated to C57BL/6NTac stud males. Embryos were harvest at the 2-cell stage (embryonic day e1.5). DNA fragments (pCMV-β-gal control and pCMV-DNBR-HA) were gel purified, filtered through 0.22μm filters, and injected at 1.5ng/μl concentration and 1ng/μl, respectively, into the cytoplasm of each blastomere. After microinjections, embryos were transferred in KSOMaa media, imaged, and cultured for 24 hours. To control for DNA

concentration injected, control embryos (pCMV-β only) were injected with the same total concentration of DNA injected into experimental embryos (DNBR-HA + pCMVβ).

Materials

DNBR amplicons for DNBR-HA

Forward: 5'-
TTTTATCGATGCGGCCGCCATGCCTCAGCTATACATTTACATCAGATTATTG
GG-3'

Reverse: 5'- CCCCCATGGCTGCTTCATCCTGTTCCAAATCACGATTGTAAC-3'

DNBR-HA into pCMV

Forward: 5'- ACCTCCCCCTGAACCTGAAA-3'

Reverse: 5'-CGGTGGGAGGTCTATATAAGCAGAGCT-3'

Oligos for generating pCS2+_P2A_mcherry

Forward: 5'-
CTGAAGCTTGGGCCCGGAAGCGGAGCTACTAACTTCAGCCTGCTGAAGCA
GGCTGGAGACGTGGAGGAGACCCTGGACCTGCGGATCCCTG-3'

Reverse: 5’-

CAGGGATCCGCAGGTCCAGGGTTCTCCTCCACGTCTCCAGCCTGCTTCAGC

AGGCTGAAGTTAGTAGCTCCGCTTCCGGGCCCAAGCTTCAG-3’

qPCR primer sequences for Id genes:

Id1

Forward: 5’- GACATGAACGGCTGCTACTCAC -3’

Reverse: 5’- GACTTCAGACTCCGAGTTCAGC -3’

Id2

Forward: 5’- GTGAGGTCCGTTAGGAAAAACAG -3’

Reverse: 5’- GTCGTTCATGTTGTAGAGCAGACT -3’

Id3

Forward: 5’- CTGTCGGAACGTAGCCTGG -3’

Reverse: 5’- GTGGTTCATGTCGTCCAAGAG -3’